

Hot-medium effects on Υ yields in p-Pb and Pb-Pb collisions

Georg Wolschin
Heidelberg University
Institut für Theoretische Physik
Philosophenweg 12-16
D-69120 Heidelberg



Heidelberg_8/2019

Topics

1. Introduction

2. Bottomonium suppression in **Pb-Pb** @ LHC

3. Our model for Υ dissociation in the QGP

4. Comparison **Pb-Pb** with p_T - and centrality-dependent CMS data

5. Cold nuclear matter (CNM) and QGP effects in 8.16 TeV **p-Pb**

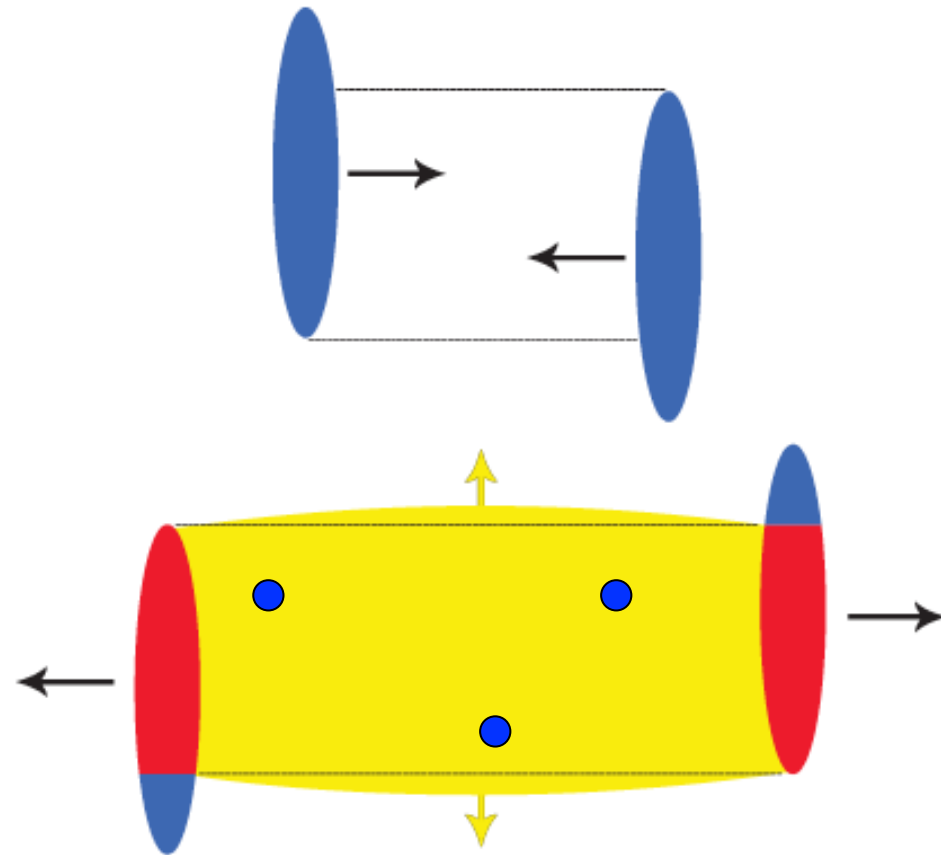
6. Comparison **p-Pb** with LHCb and ALICE data

7. Conclusion

1.Intro: Quark-gluon plasma (QGP) and heavy quarkonia

... is being created in relativistic heavy-ion collisions in the mid-rapidity gluon-gluon source, and in the fragmentation sources provided the spatial overlap is sufficiently strong

Red: fragmentation sources



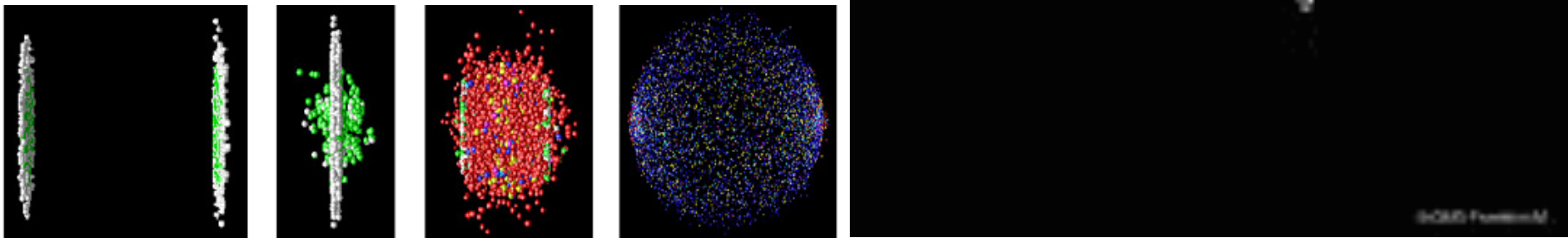
● Heavy quarkonia in the QGP of gluons and light (u, d, s) quarks

graphic from: B. Kellers&GW, PTEP 2019, 053 (2019)

Time-dependent
simulation:

**Quark-gluon plasma (QGP) created in relativistic
heavy-ion collisions**

$t_{\text{int}} \approx 5-8 \text{ fm}/c$ @ LHC



© CERN

In the first stages of the collision, **gluons** equilibrate, **quarks** and **heavy quarkonia** form, later more matter and antimatter is being created from the relativistic energy in the **fireball**, $E = \sqrt{(p^2 + m^2)}$, it expands and cools, then hadronizes completely. Created baryons, mesons (or their decay products), photons, leptons are then detected:

→ Conclusions regarding the QGP properties are drawn.

Large Hadron Collider (LHC) / CERN



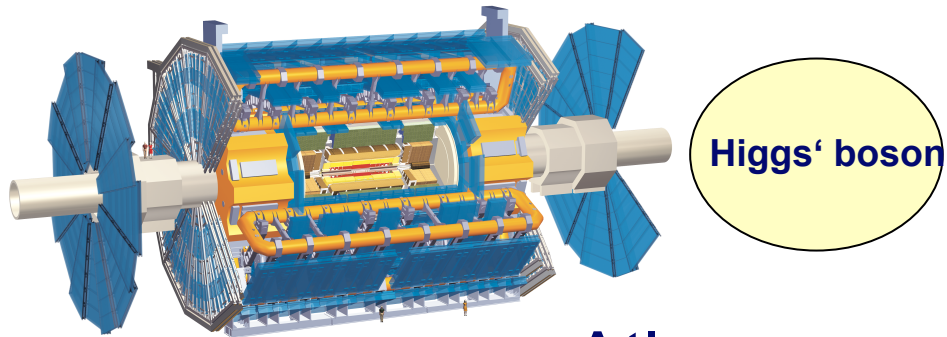
p+p @ 7,8,13,(14) TeV

p+Pb @ 5.02 TeV 2012/13
@ 5.02, 8.16 TeV Nov. 2016

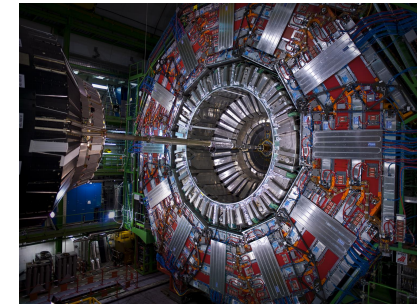
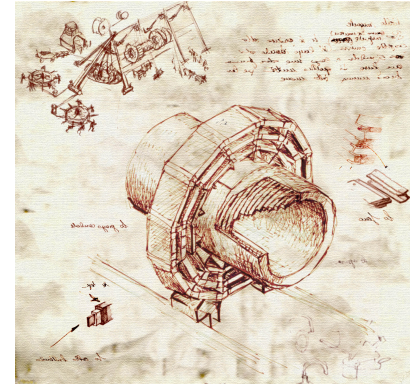
Pb+Pb @ 2.76 TeV 2011/12 Run 1
@ 5.02 TeV Nov. 2015 Run 2
Nov. 2018 Run 2

(design energy 5.52 TeV)

LHC Detectors: pp,
plus Relativistic heavy-ion physics: **Pb-Pb**, **p-Pb**

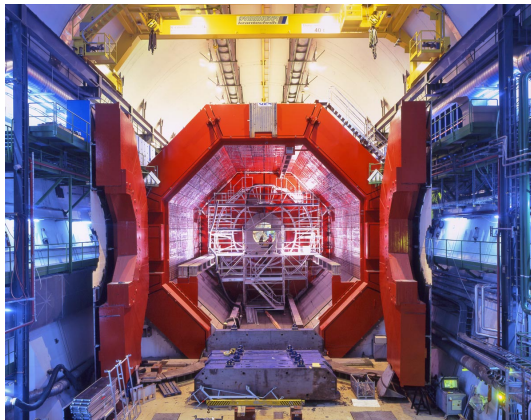


Atlas
≈ 35 HI people



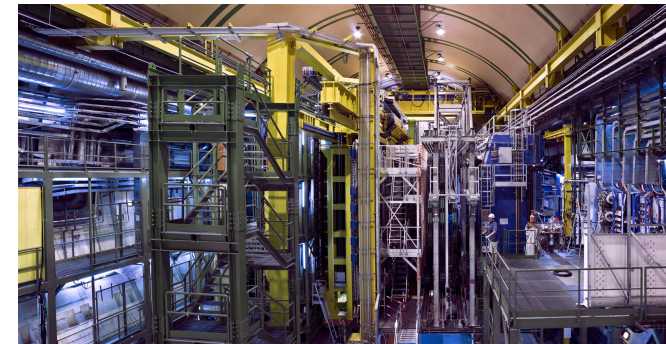
CMS
da Vinci style

≈ 60 HI people
Pb-Pb, **p-Pb**



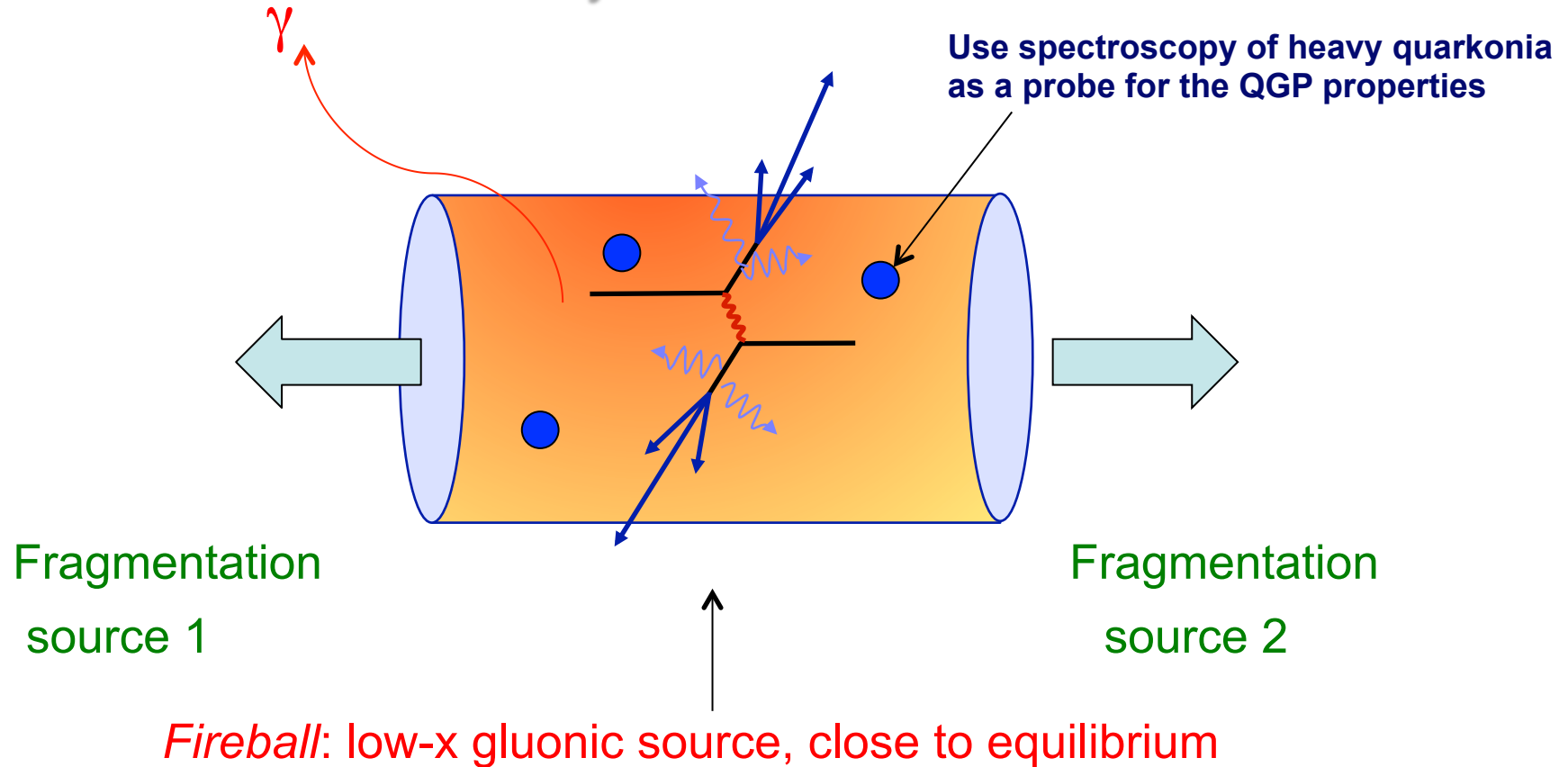
Alice: L3 magnet
> 1,000 HI people

Pb-Pb
p-Pb



LHCb
p-Pb; **peripheral PbPb**

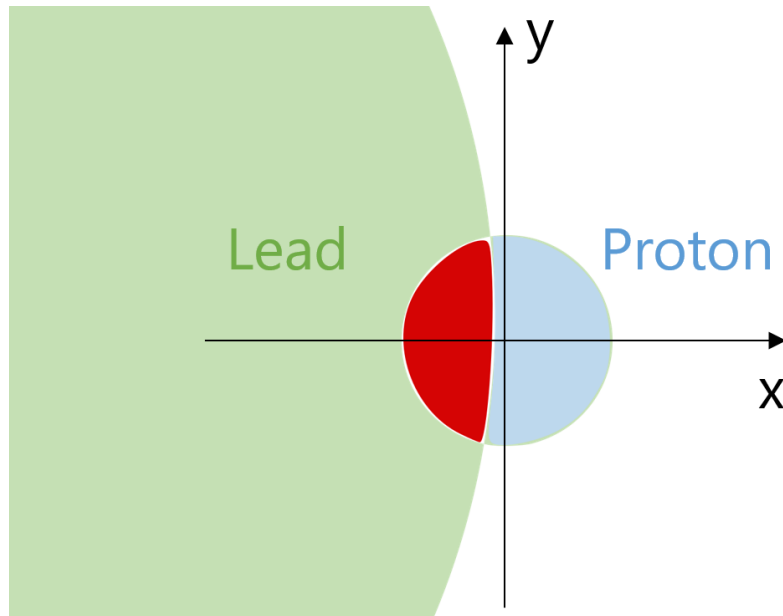
Three sources for particle production in a symmetric relativistic heavy-ion collision such as Pb-Pb



Particle production in the midrapidity source is often considered in a **Thermal Model with a limiting temperature T_H** (which dates back to R. Hagedorn of CERN) – in spite of the short interaction time of $\sim 10^{-23}$ s

Asymmetric p-Pb collisions

Overlap of the thickness functions θ in the transverse plane



Thickness functions

$$\theta_p(b; x^1, x^2) = \int dx^3 \rho_p(|b\vec{e}_1 - \vec{x}|),$$

$$\theta_{Pb}(b; x^1, x^2) = \int dx^3 \rho_{Pb}(|\vec{x}|),$$

Overlap function

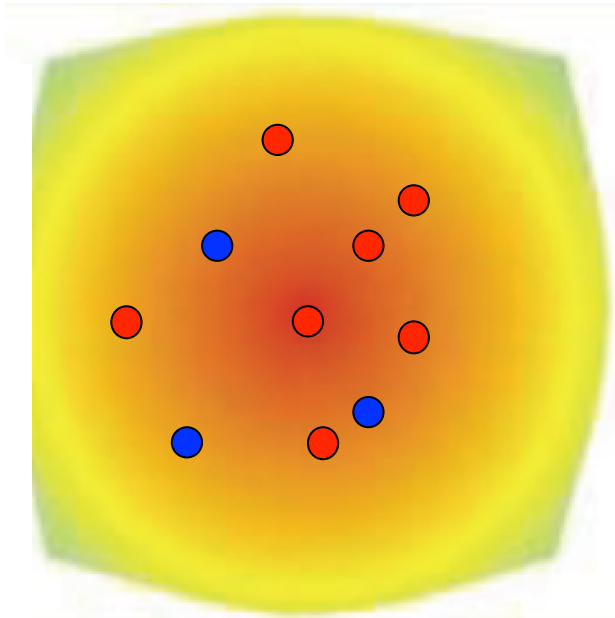
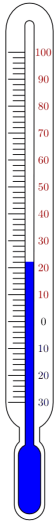
$$\theta_{pPb}(b; x^1, x^2) = \theta_p(b; x^1, x^2) \times \theta_{Pb}(b; x^1, x^2)$$

graphic from: V.H. Dinh, MSc thesis, Heidelberg (2019)

(In the transverse plane)

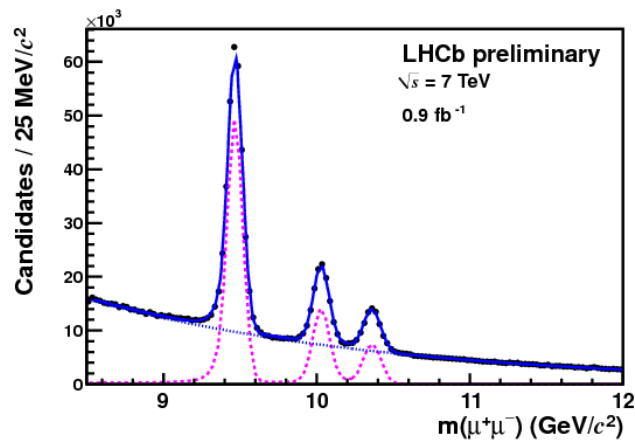
Most of the system remains 'cold': $T < T_H$
 \Rightarrow Consider CNM effects on Y yields,
plus suppression in the hot QGP

2. Heavy quarkonia in the QGP



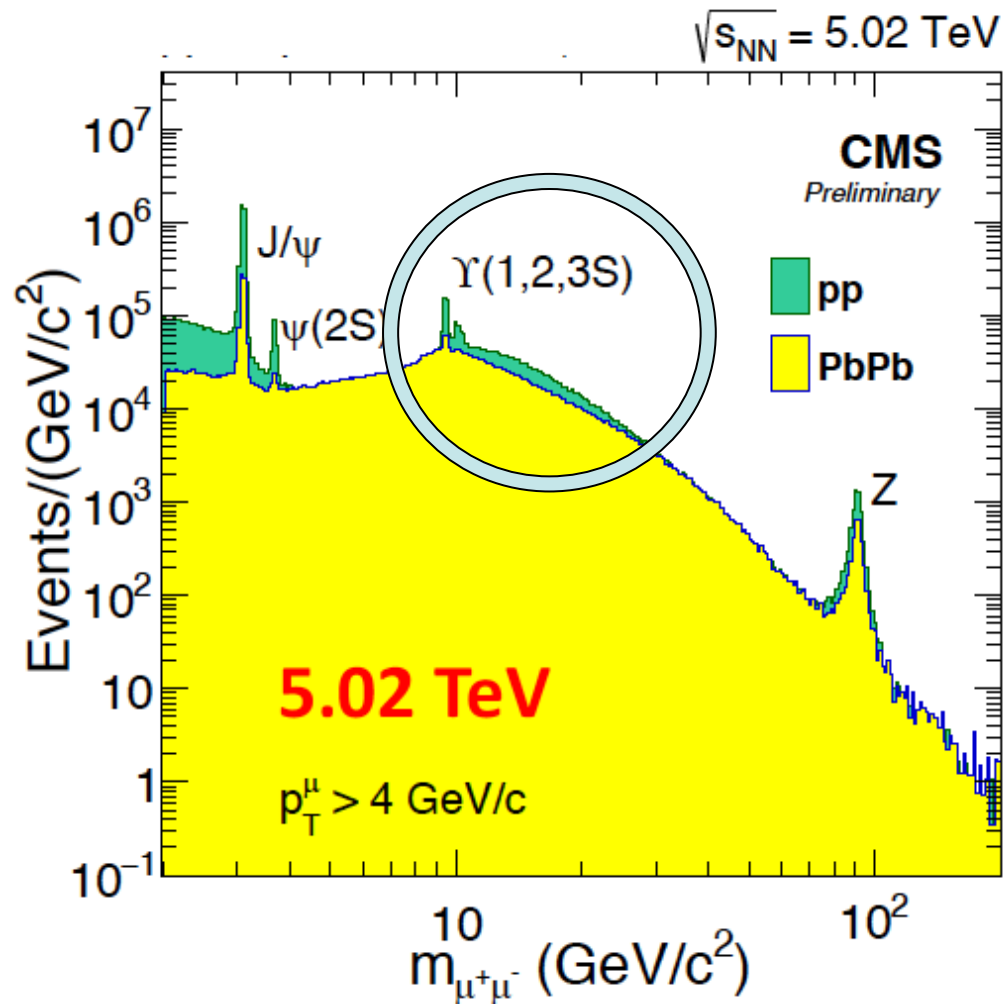
- J/ψ ($c\bar{c}$)
- Υ ($b\bar{b}$)

- Investigate their spectroscopy in the QGP
- Deduce QGP properties such as the temperature T : “QGP-Thermometer“
- Focus on Υ because there, recombination is negligible



Υ spectrum in vacuum \Rightarrow in the QGP medium?

Υ suppression in PbPb @ LHC



Υ suppression as a sensitive probe for the QGP

- No significant effect of regeneration
- $m_b \approx 3m_c \Rightarrow$ cleaner theoretical treatment
- More stable than J/ψ

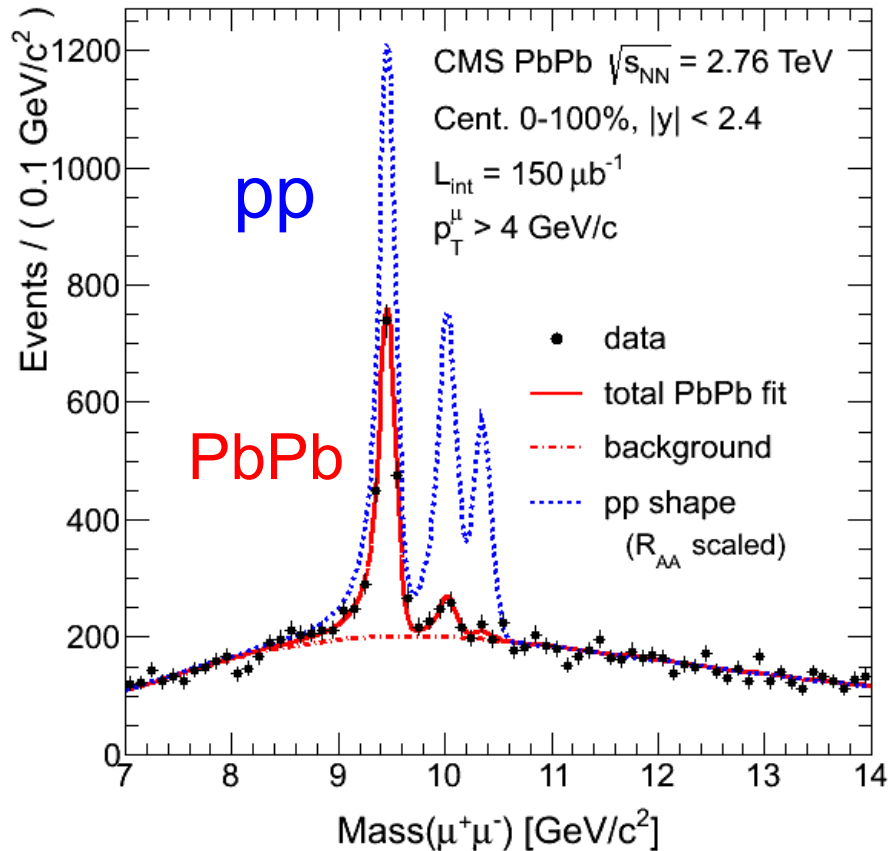
$$E_B(\Upsilon_{1S}) \approx 1.10 \text{ GeV}$$

$$E_B(J/\psi) \approx 0.64 \text{ GeV}$$

Use $\Upsilon_{1S, 2S, 3S}$ for spectroscopy in the QGP

Y(nS) states are suppressed in PbPb @ LHC:

CMS



Y spectroscopy as
a clear QGP indicator

1. Y(1S) ground state is suppressed in PbPb:

$$R_{AA}(Y(1S)) = 0.56 \pm 0.08 \pm 0.07 \text{ in min. bias}$$

2. Y(2S, 3S) states are > 4 times more suppressed in PbPb than Y(1S)

$$R_{AA}(Y(2S)) = 0.12 \pm 0.04 \text{ (stat.)} \pm 0.02 \text{ (syst.)}$$

$$R_{AA}(Y(3S)) = 0.03 \pm 0.04 \text{ (stat.)} \pm 0.01 \text{ (syst.)}$$

$$R_{AA} = \frac{N_{PbPb}(Q\bar{Q})}{N_{coll}N_{pp}(Q\bar{Q})}$$

© CMS Collab., PRL 109, 222301 (2012)
[Plot from CMS database]

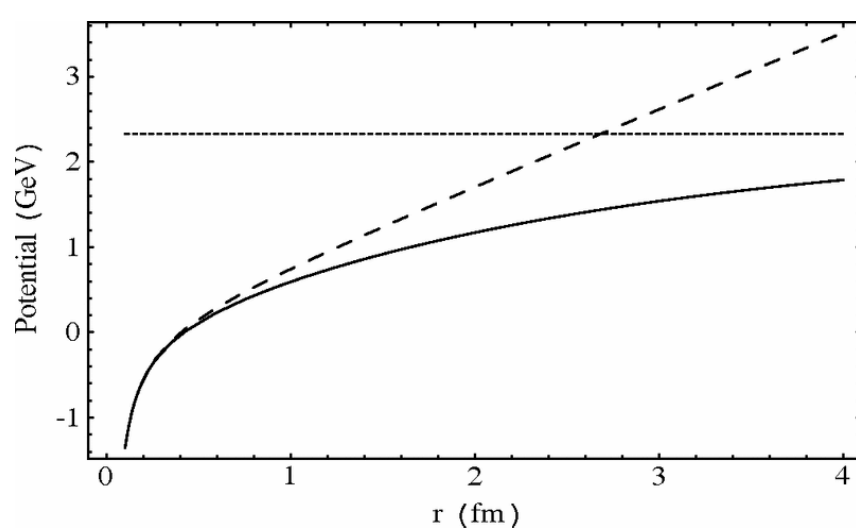
3. The model: Screening, Gluodissociation and Collisional broadening of the $Y(nS)$ states

- ① Debye screening of all states involved: **Static suppression**
- ② The **imaginary part** of the potential (effect of collisions) contributes to the broadening of the $Y(nS)$ states: **damping**
- ③ **Gluon-induced dissociation: dynamic suppression**, in particular of the $Y(1S)$ ground state due to the large thermal gluon density
- ④ **Reduced feed-down** from the excited Y/χ_b states to $Y(1S)$ substantially modifies the populations: **indirect suppression**

J. Hoelck, F. Nendzig and GW, Phys. Rev. C 95, 024905 (2017); J. Hoelck and GW, EPJA 53, 37 (2017)
F. Vaccaro, F. Nendzig and GW, EPL102, 42001 (2013); F. Nendzig and GW, Phys. Rev. C 87, 024911 (2013);
J. Phys. G41, 095003 (2014); F. Brezinski and GW, Phys. Lett.B 70, 534 (2012)

① Screening in a nonrelativistic potential model

Proposal **Matsui&Satz 1986**: At high temperatures in the Quark-Gluon medium, the Cornell-type **real quark-antiquark potential** is ‘screened’, analogously to the Debye screening in an electromagnetic plasma



$$V_{\text{Cornell}}(r) = (\sigma r - \kappa/r)$$

$$V_{\text{screened}}(r) = -\frac{\kappa}{r}e^{-r/\lambda_D} + \sigma\lambda_D(1 - e^{-r/\lambda_D})$$

σ string tension, κ Coulomb-parameter

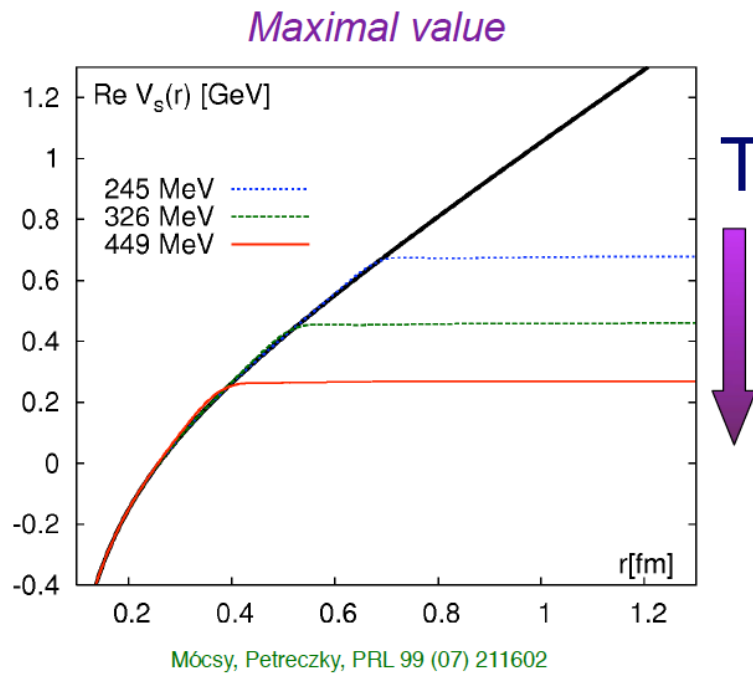
λ_D = Debye length, T = temperature

=> Heavy mesons can “melt” in the hot medium

② Optical quark-antiquark potential:

Screened real part, T-dep. imag. part

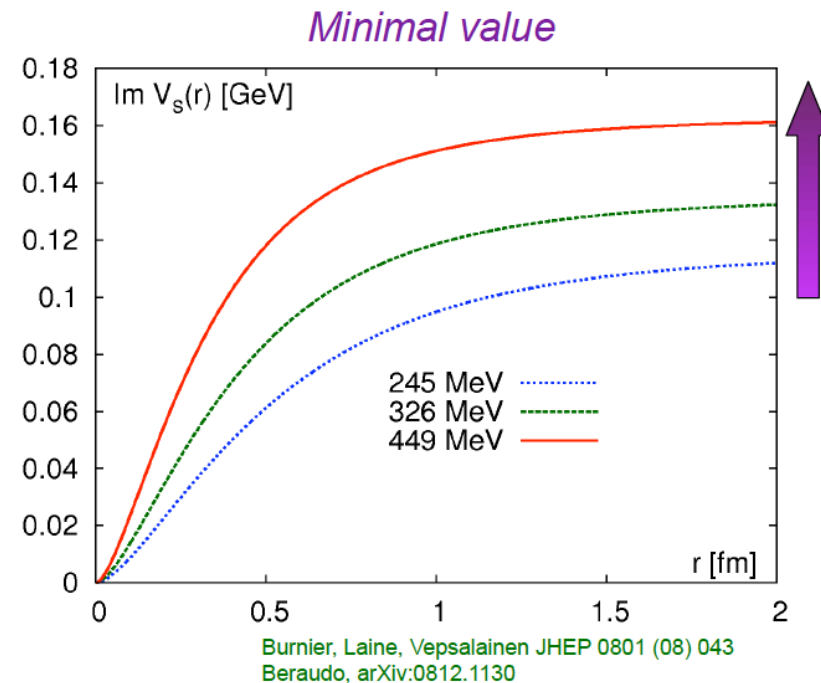
Constrain $\text{Re}V_s(r)$ by lattice QCD data on the singlet free energy



Screening

From: A. Mocsy et al.

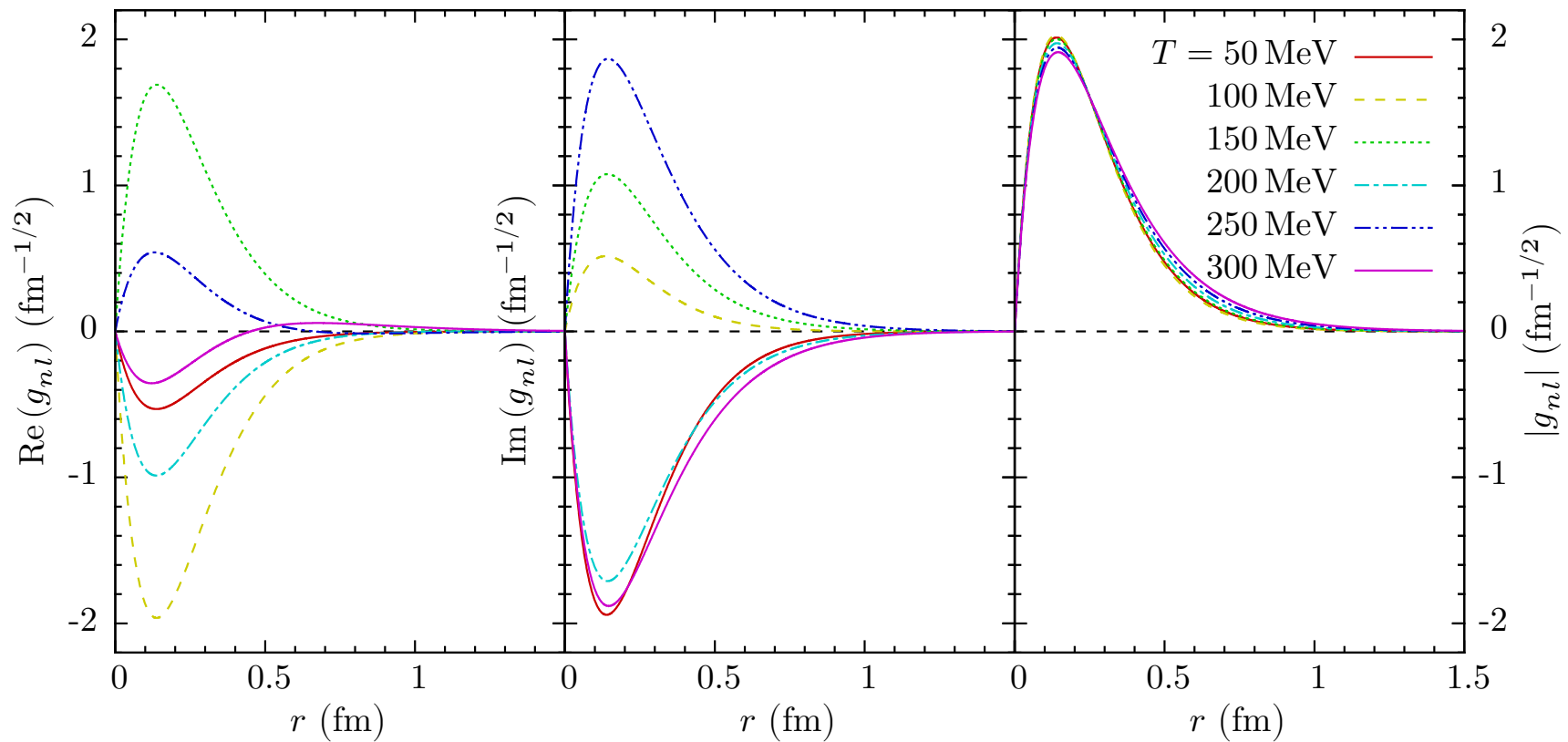
Take $\text{Im}V_s(r)$ from pQCD calculations



Damping

Radial wave function of $Y(1S)$ at temperatures T

Solutions of the Schrödinger equation with complex potential $V(r, T, \alpha_s)$ for the radial wave functions $g_{nl}(r, T)$, $[H(r, T, \alpha_s) - E + i\Gamma/2]g(r) = 0$



③ Gluon-induced dissociation of heavy mesons in the QGP

Born amplitude for the interaction of gluon clusters according to Bhanot&Peskin in dipole approximation / Operator product expansion, extended to include the screened coulombic + string eigenfunctions as outlined in Brezinski and Wolschin, PLB 70, 534 (2012)

$$\sigma_{diss}^{nS}(E) = \frac{2\pi^2 \alpha_s E}{9} \int_0^\infty dk \delta\left(\frac{k^2}{m_b} + \epsilon_n - E\right) |w^{nS}(k)|^2$$
$$w^{nS}(k) = \int_0^\infty dr r g_{n0}^s(r) g_{k1}^a(r)$$

for the Gluodissociation cross section of the $Y(nS)$ states, and correspondingly for the $\chi_b(nP)$ states.

Gluodissociation cross section

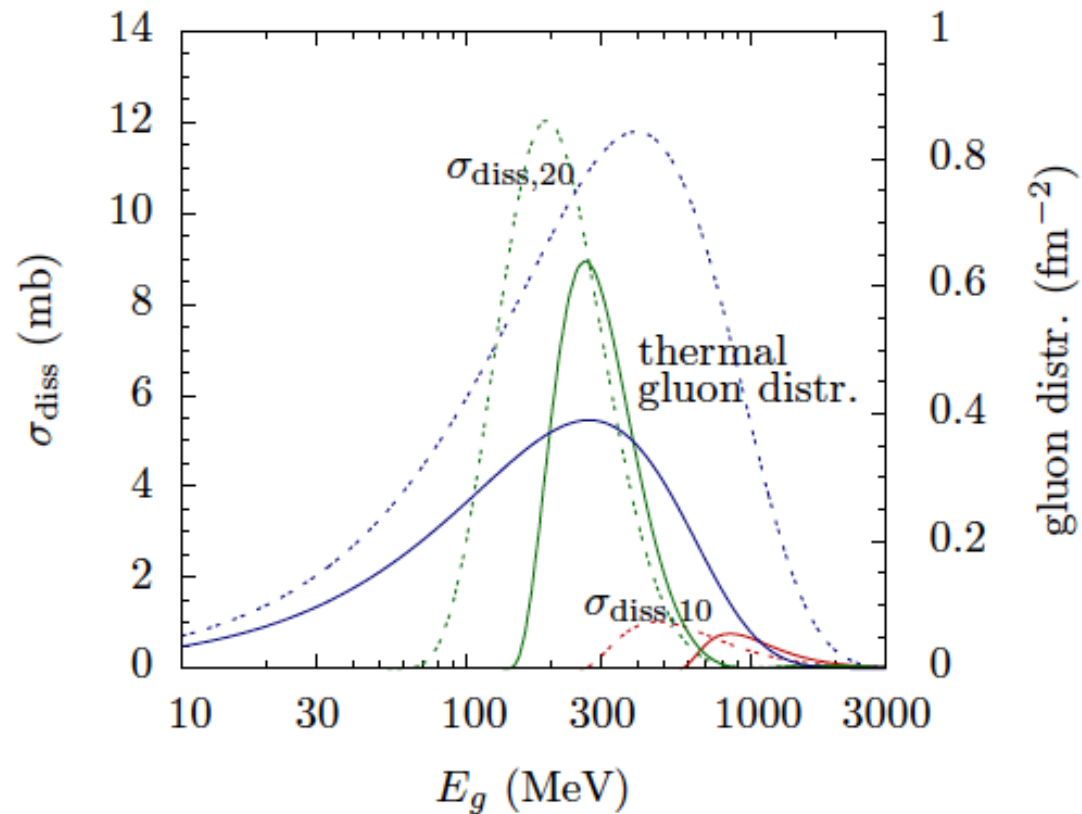


Figure 3. Gluodissociation cross section σ_{diss} (left scale) of the $\Upsilon(1S)$ and $\Upsilon(2S)$ and the thermal gluon distribution (right scale) plotted for temperature $T = 170$ (solid curves) and 250 MeV (dotted curves) as functions of the gluon energy E_g .

F. Nendzig and GW, J. Phys. G41, 095003 (2014)

Heidelberg_8/2019

Thermal gluodissociation cross section

Average the gluodissociation cross section over the Bose-Einstein distribution of the thermal gluons in the QGP to obtain the dissociation width at temperature T for each of the six bottomia states involved

$$\Gamma_{\text{diss}, nl}(T) \equiv \frac{g_d}{2\pi^2} \int_0^\infty \frac{dE_g E_g^2 \sigma_{\text{diss}, nl}(E_g)}{e^{E_g/T} - 1}$$

$$(g_d = 16)$$

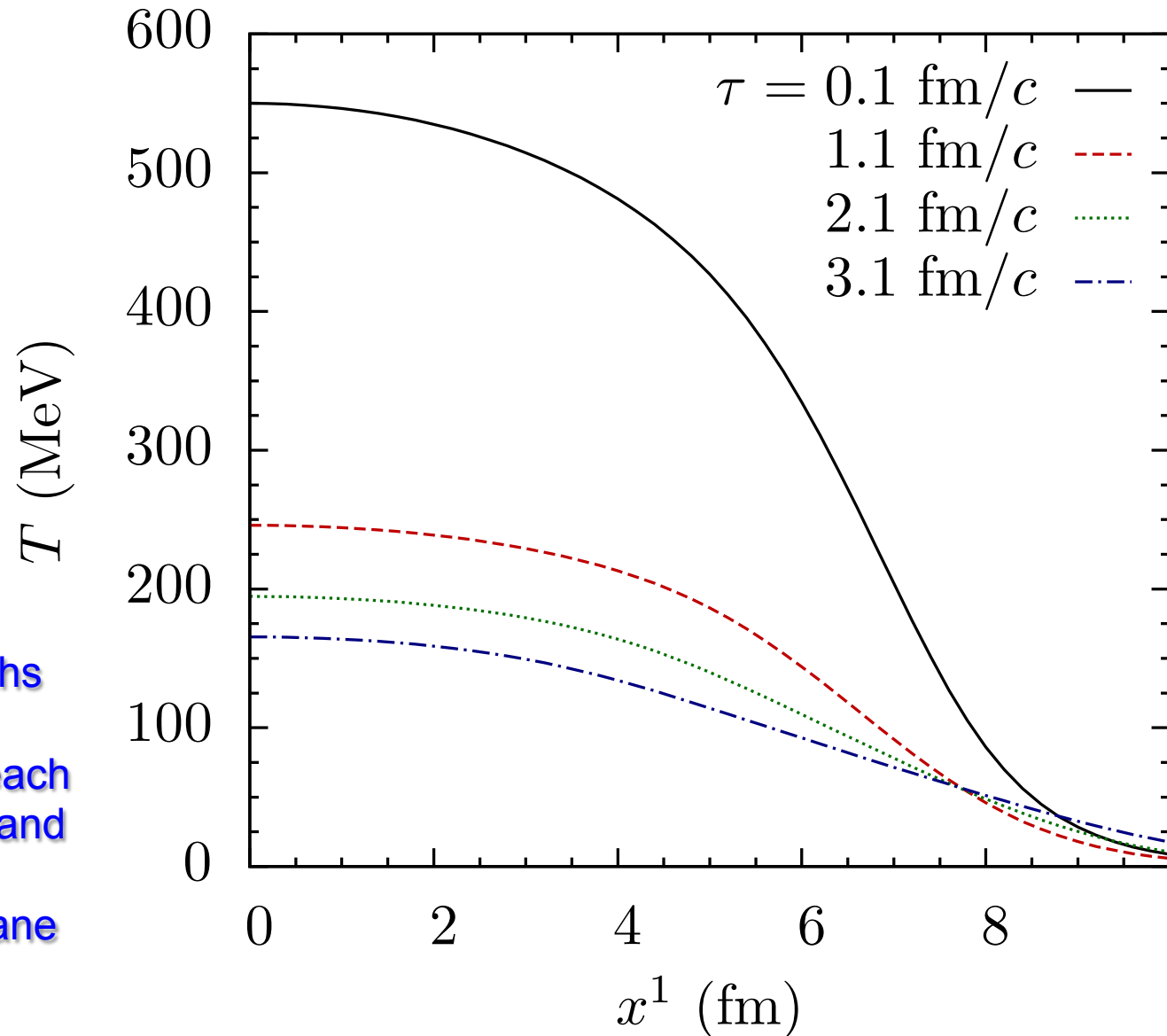
With rising temperature, the peak of the gluon distribution moves to larger gluon energies E_g , whereas the dissociation cross sections move to smaller E_g , giving rise to a maximum in the gluodissociation width for fixed coupling α_s . (Larger cross sections at higher temperatures due to **running coupling** counteract.)

$$\Gamma_{\text{tot}}^{nl}(T) = \Gamma_{\text{damp}}^{nl}(T) + \Gamma_{\text{diss}}^{nl}(T)$$

Hydrodynamic expansion (ideal)

Temperature profile for central collisions at different times τ

Use total decay widths $\Gamma_{\text{tot}}(b, x^1, x^2)$ of the bottomonia states for each impact parameter b and time step t in the transverse (x^1, x^2) plane



Dynamical fireball evolution

Dependence of the local temperature T on impact parameter b , time t , and transverse coordinates x, y evaluated in ideal hydrodynamic calculation with transverse expansion

$$T(b, \tau_{init}, x^1, x^2) = T_0 \left(\frac{N_{mix}(b, x^1, x^2)}{N_{mix}(0, 0, 0)} \right)^{1/3}$$

$$N_{mix} = \frac{1-f}{2} N_{part} + f N_{coll}, \quad f = 0.145$$

The number of produced $b\bar{b}$ -pairs is proportional to the number of binary collision, and the nuclear overlap

$$N_{b\bar{b}}(b, x, y) \propto N_{coll}(b, x, y) \propto T_{AA}(b, x, y)$$

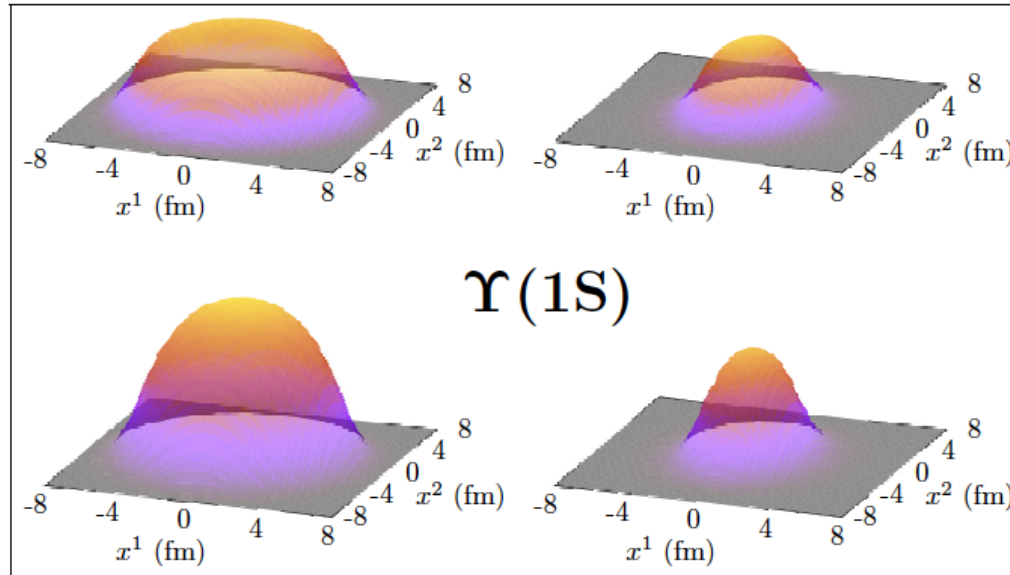
QGP suppression factor (without feed-down and CNM effects):

$$R_{AA}^{QGP} = \frac{\int d^2b \int dx dy T_{AA}(b, x, y) e^{-\int_{t_F}^{\infty} dt \Gamma_{tot}(b, t, x, y)}}{\int d^2b \int dx dy T_{AA}(b, x, y)}$$

Integrand
in the
transverse
plane

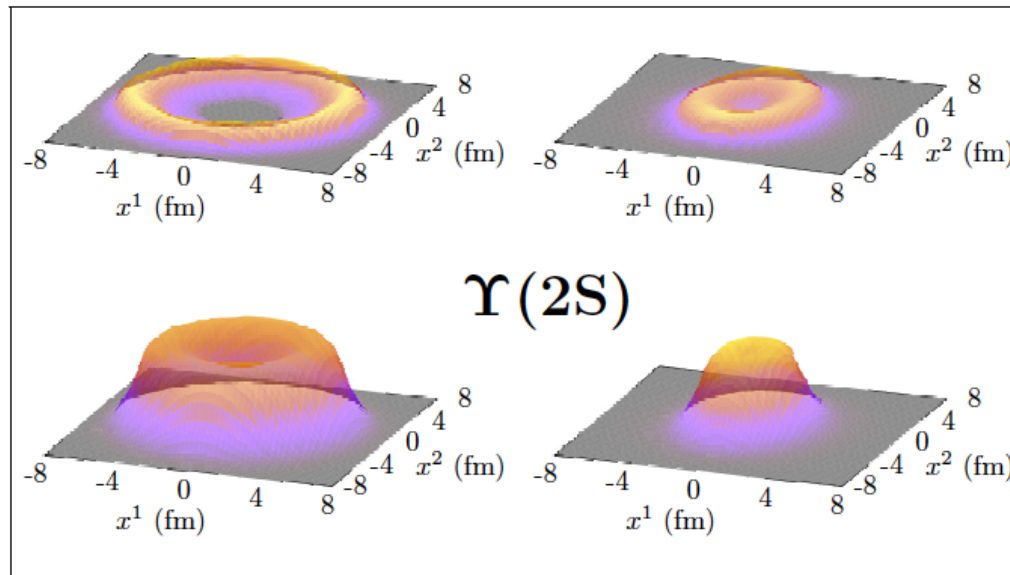
$b = 0 \text{ fm}$

$b = 8 \text{ fm}$



$p_T = 0$

$p_T = 12 \text{ GeV}/c$



$p_T = 0$

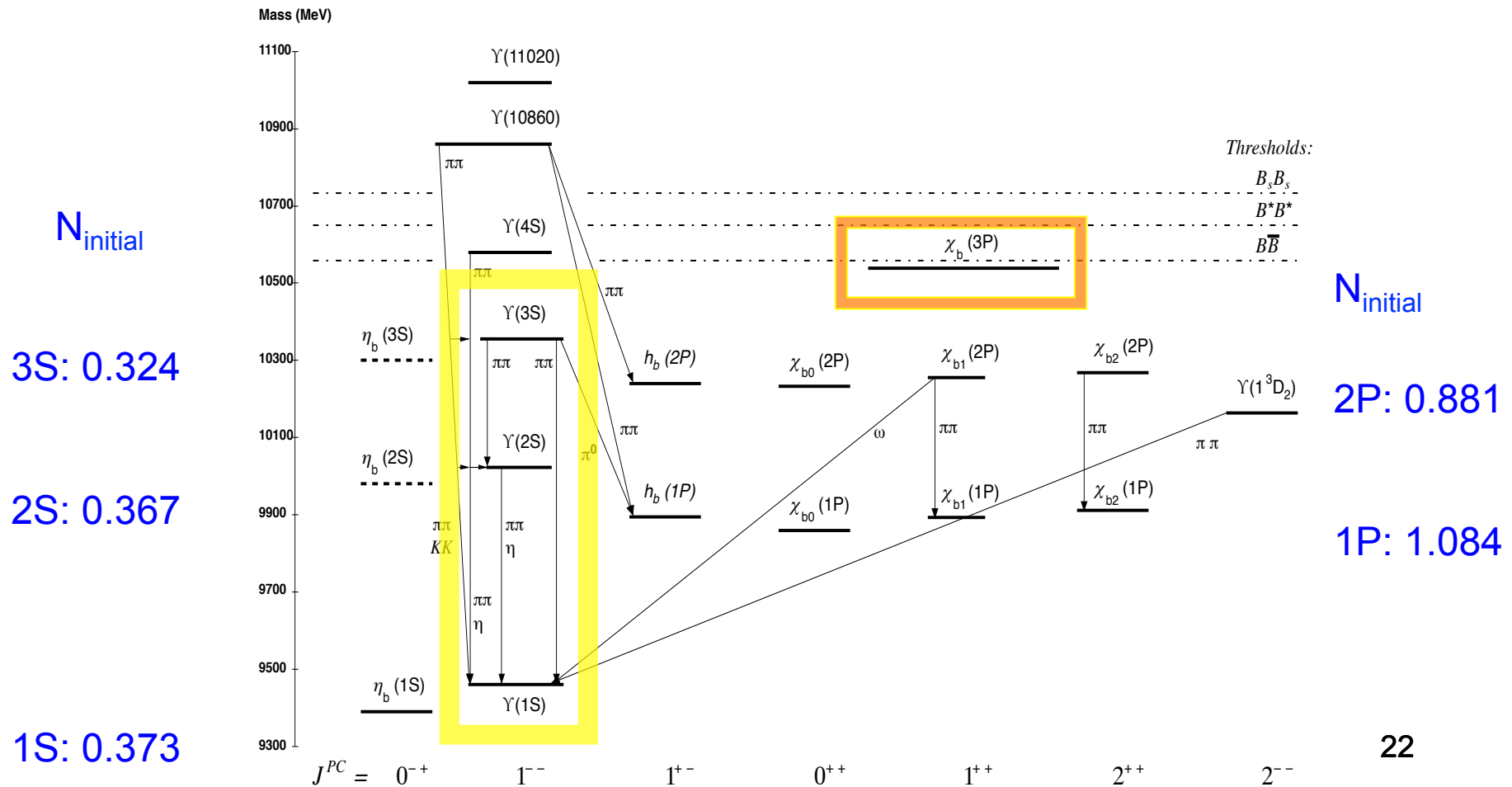
$p_T = 12 \text{ GeV}/c$

Nendzig&GW,
J. Phys. G41,
095003 (2014)

④ Feed-down cascade

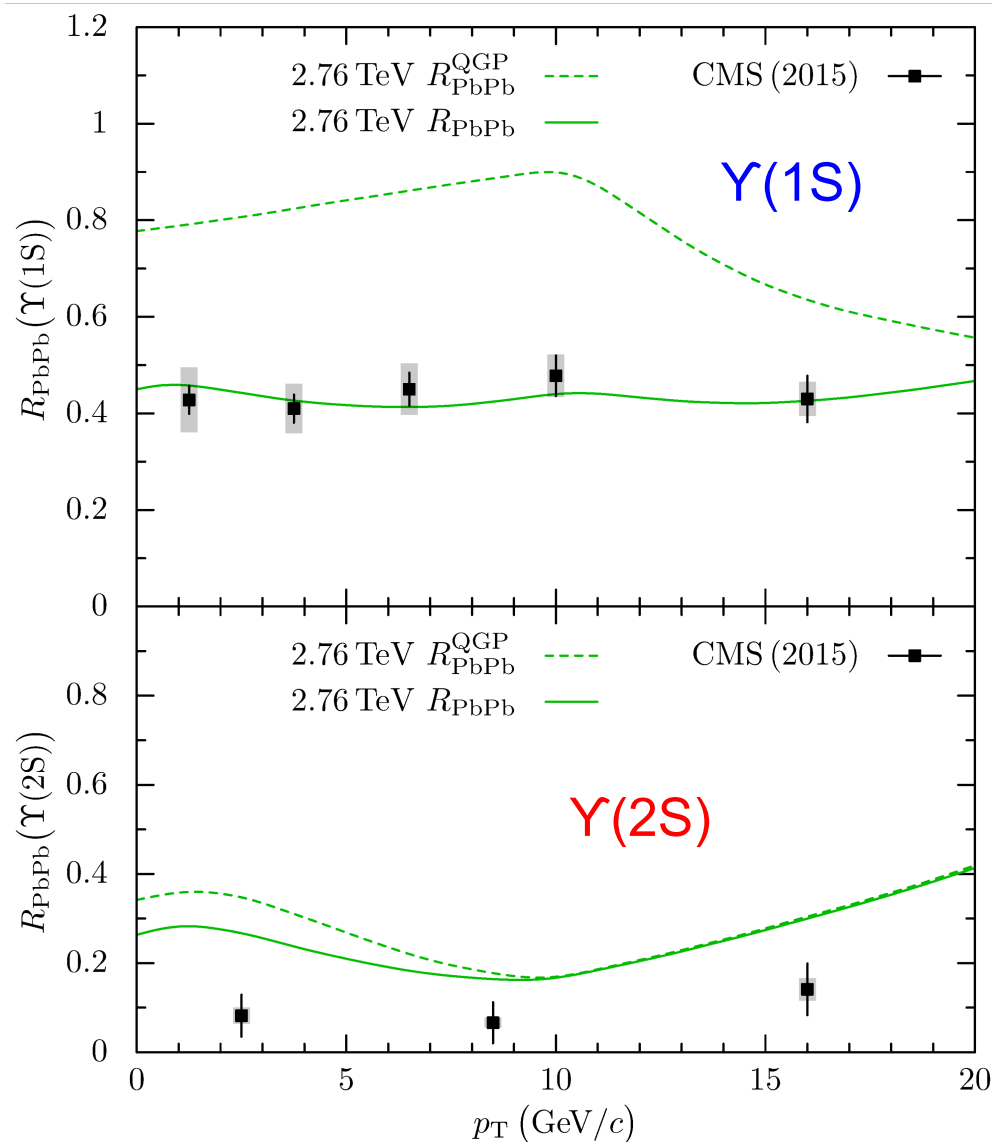
including χ_{nP} states; relative initial populations in pp computed using an inverted cascade from the final populations measured by CMS and CDF(χ_b).

Feed-down is reduced if excited states are screened or depopulated



4.1 Selected results Pb-Pb vs. CMS data:

Transverse-momentum dependence of $\Upsilon(1S)$ suppression in PbPb at 2.76 TeV



The $\Upsilon(1S)$ suppression is mostly reduced feed-down (31% in-medium), the $\Upsilon(2S)$ suppression primarily in-medium (94% in min. bias)

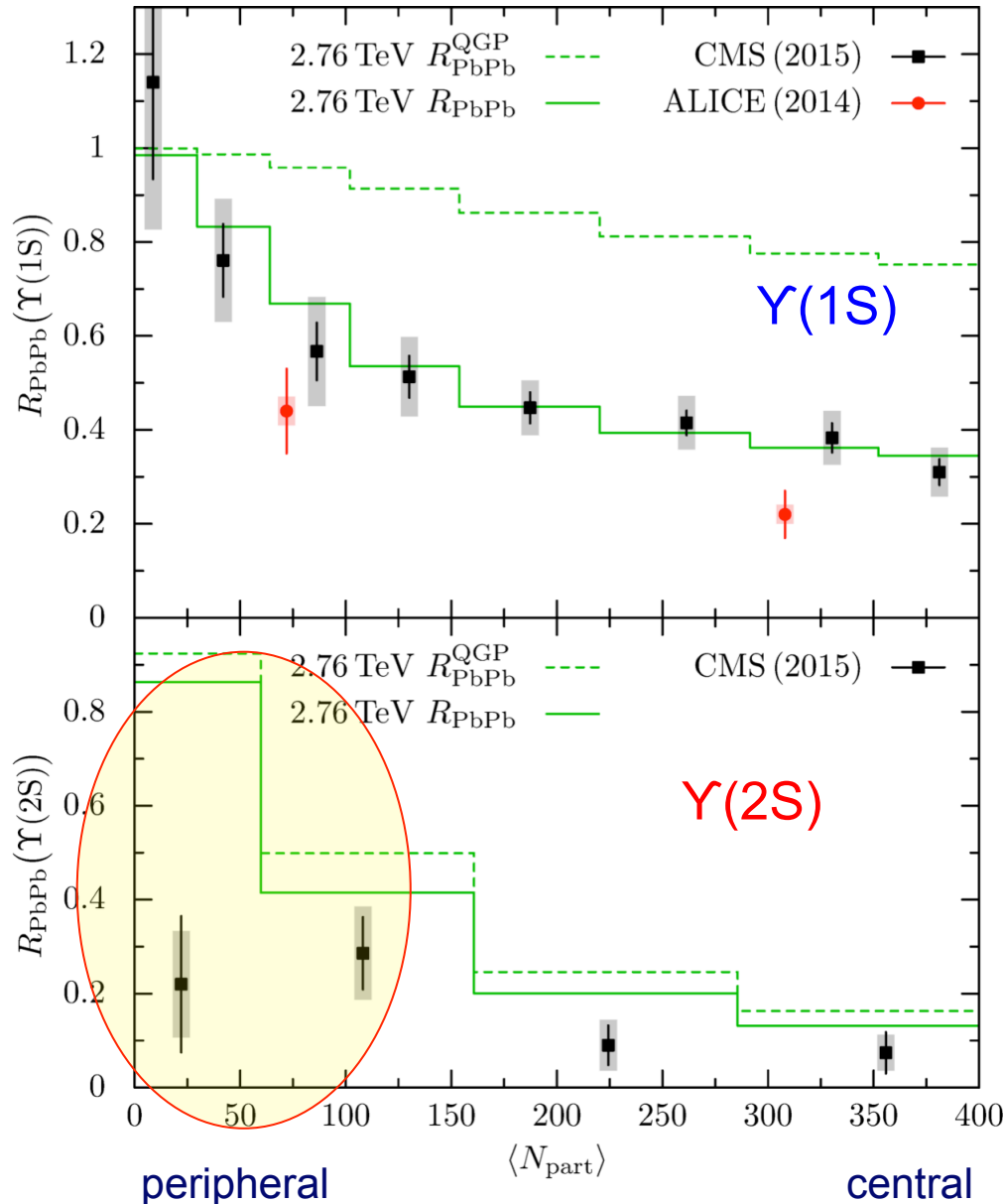
← In-medium suppression only
 ← Including reduced feed-down

($T_0 = 480$ MeV; $t_F = 0.4$ fm/c;
 CMS data 2015)

J. Hoelck, F. Nendzig and GW,
 Phys. Rev. C 95, 024905 (2017)

Reduced feed-down only relevant
 for $\Upsilon(1S)$, not for excited states

2.76 TeV Pb-Pb centrality-dependent results vs. CMS and ALICE



2.76 TeV PbPb LHC

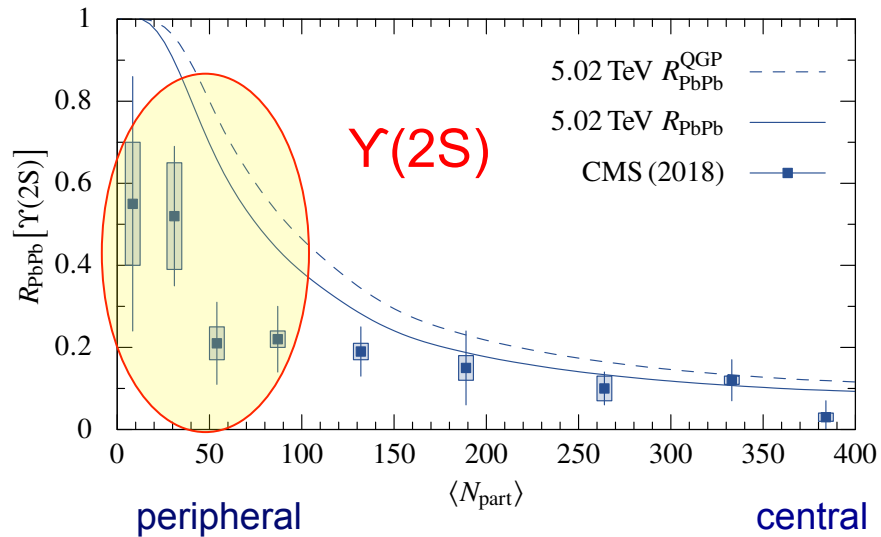
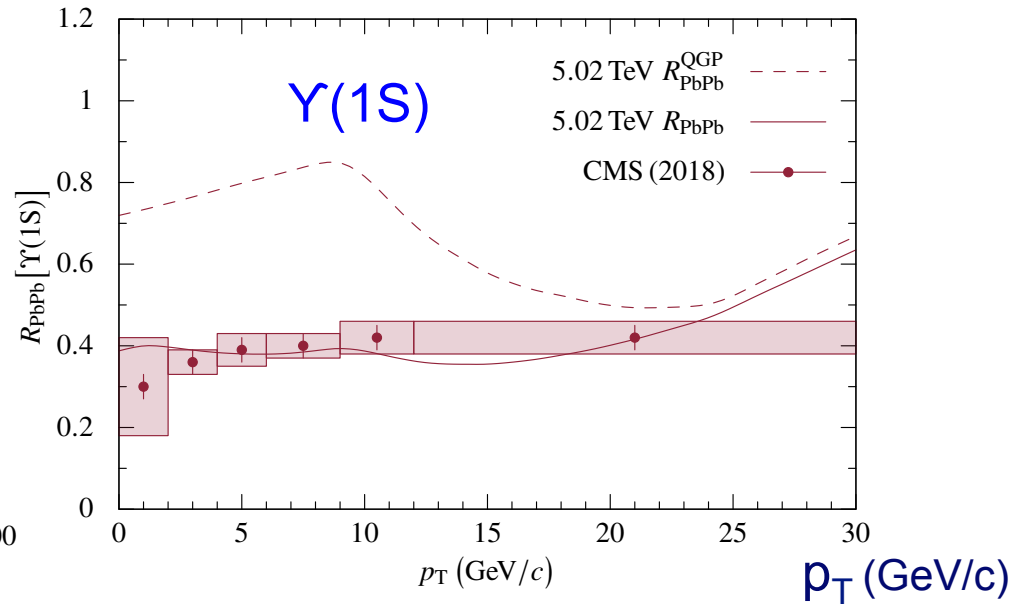
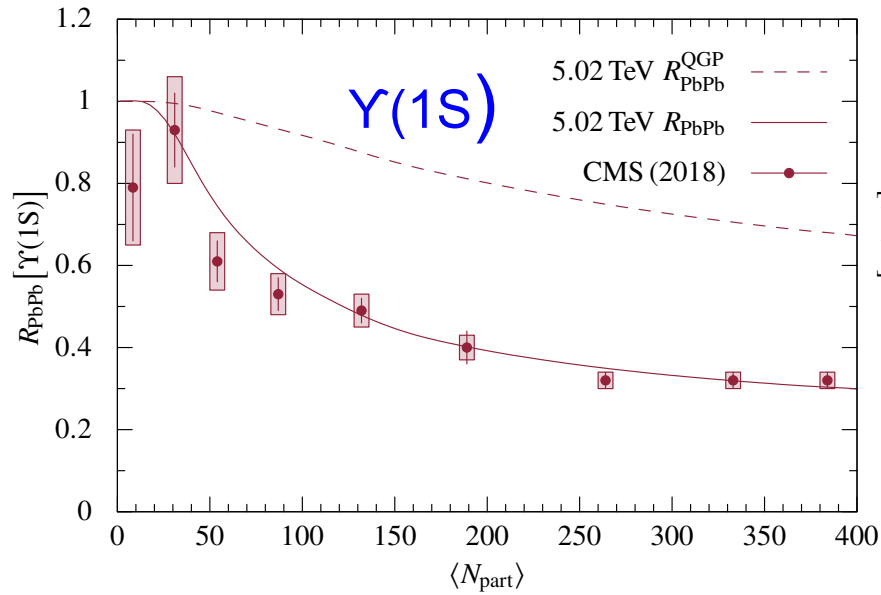
$t_F = 0.4$ fm/c: Υ formation time

$T_0 = 480$ MeV: central temp.
 at $b = 0$ and $t = t_F$

Room for **additional suppression mechanisms** for the excited states:
Hadronic dissociation, mostly by pions, is one possibility. **Thermal pions** are insufficient; **direct pions** may contribute, and **magnetic dissociation**.

J. Hoelck, F. Nendzig and GW,
 Phys. Rev. C 95, 024905 (2017)

4.2 Prediction for Υ suppression in 5.02 TeV PbPb vs. CMS data



Predictions (dashed/ solid curves) as calculated in

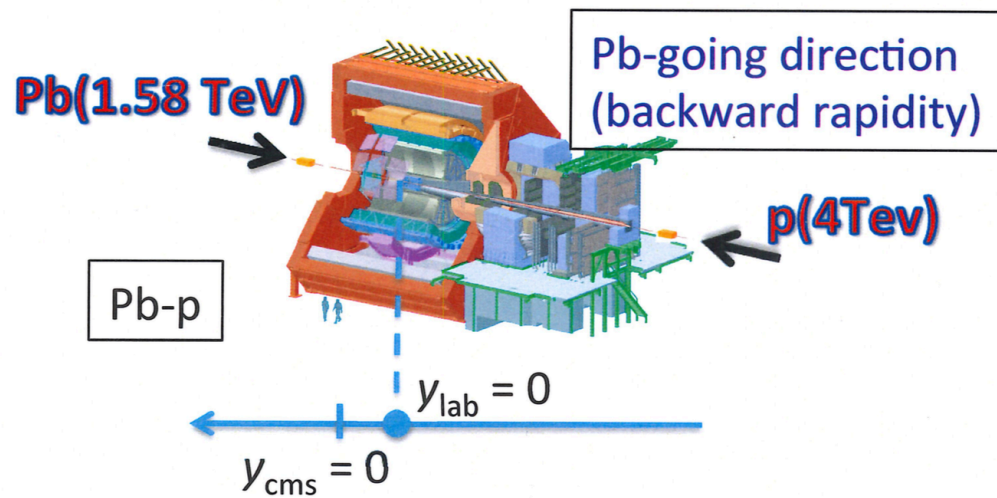
**J. Hoelck, F. Nendzig and GW,
Phys. Rev. C 95, 024905 (2017)**

CMS data: Phys. Lett. B 790, 270 (2019)

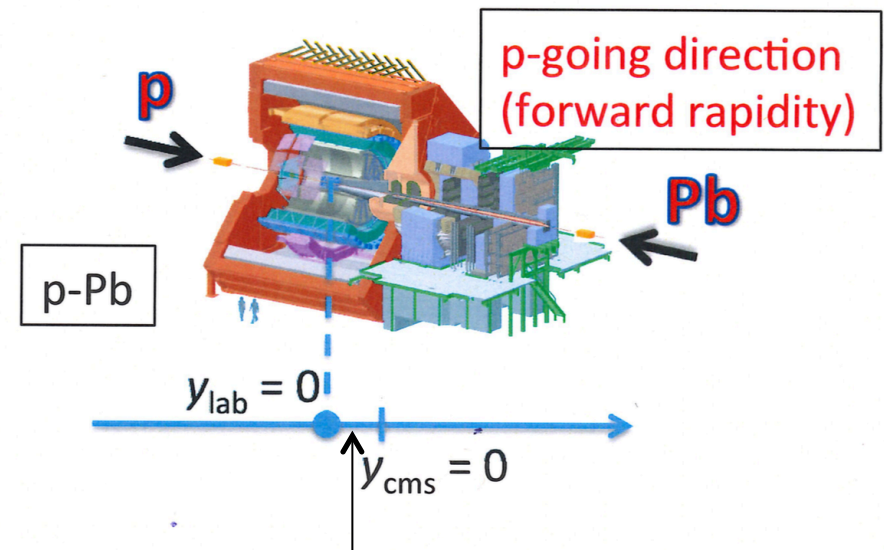
4.3. Υ in Pb-Pb @ LHC energies

- The spectroscopy of Υ mesons in PbPb collisions at LHC energies provides information about QGP properties, in particular the initial central temperature.
- The theoretical model is found to be in agreement with the CMS results for Υ (1S). Screening is not decisive for the 1S state except for central collisions.
- The Υ (1S) suppression is mostly reduced feed-down, the Υ (2S) primarily in-medium. The prediction for Υ (1S) in 5.02 TeV PbPb agrees with CMS data.
- The enhanced suppression of Υ (2S, 3S) leaves room for additional suppression mechanisms.

5. Cold-matter (CNM) and hot-medium (QGP) effects in asymmetric collisions: p-Pb

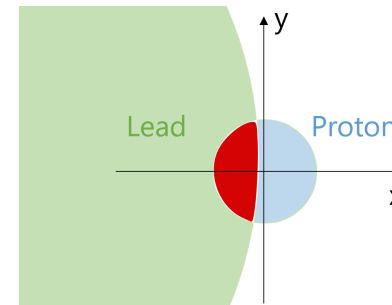


© ALICE



Rapidity shift: $\Delta y = 0.465$

p+Pb @ $\sqrt{s_{NN}} = 5.02, 8.16$ TeV



CNM and QGP effects in asymmetric collisions

- Bottomonia yields are influenced by the presence of nuclear matter: Cold nuclear matter (CNM) effects.
- This includes pure initial-state effects, such as the modification of the initial gluon densities in the nuclear medium, and
- Mixed initial- and final-state effects, such as coherent parton energy loss induced by the nuclear medium.

We consider both effects, together with the additional Υ suppression in the hot quark-gluon plasma – as in Pb-Pb.

V.H. Dinh, J. Hoelck and GW,
Phys. Rev. C, in press (2019)

Modification of bottomonium yields in p-Pb vs. pp

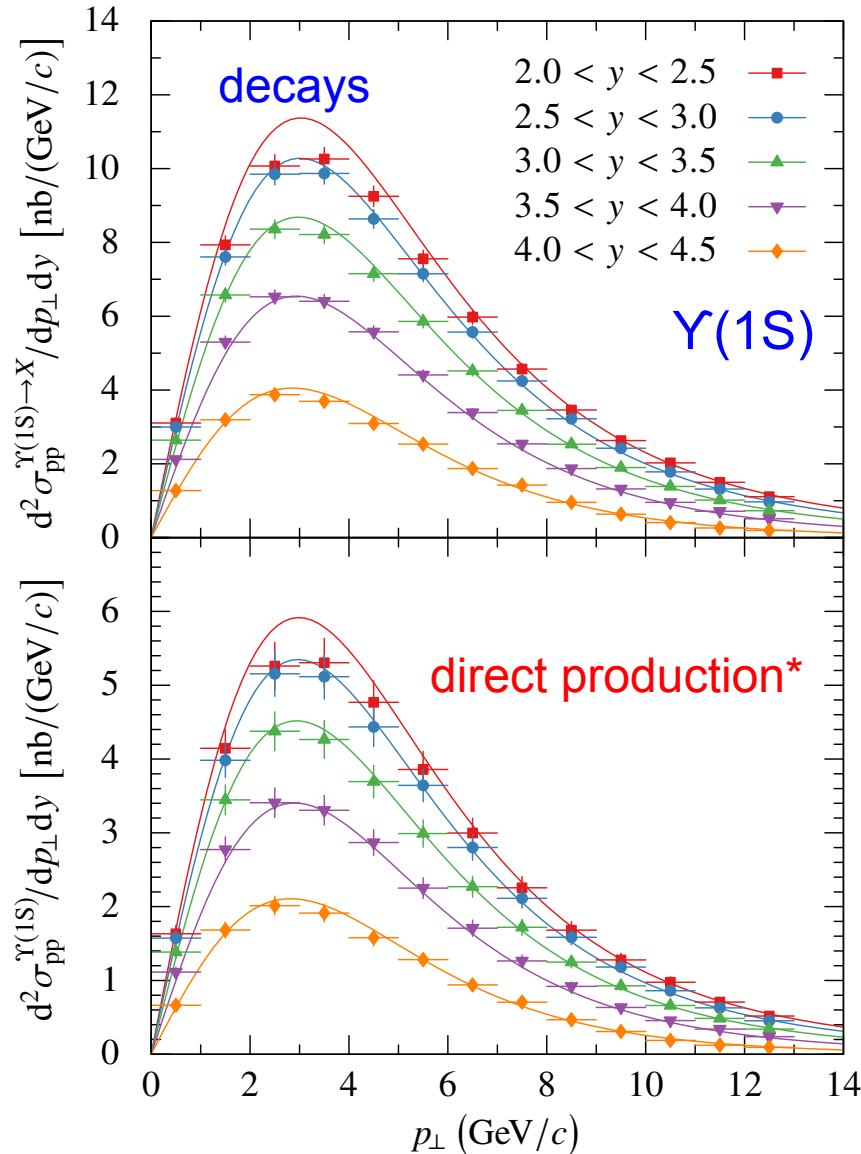
Modification factors R_{pPb} depend on rapidity y , transverse momentum p_T , and centrality / impact parameter b

$$R_{pPb}(b, p_{\perp}, y) = \frac{1}{\langle N_{\text{coll}} \rangle(b)} \frac{\frac{d^2 \sigma_{pPb}^{\Upsilon \rightarrow X}}{dp_{\perp} dy}(b, p_{\perp}, y)}{\frac{d^2 \sigma_{pp}^{\Upsilon \rightarrow X}}{dp_{\perp} dy}(p_{\perp}, y)}$$

with $d^2 \sigma^{\Upsilon \rightarrow X} / (dp_{\perp} dy)$ the Lorentz-invariant double-differential cross section for Υ decays, calculated via the decay cascade from the corresponding production after applying **CNM** and **QGP** modifications.

The Υ production cross section in pp is derived from the measured decay cross section in pp, applying an inverse feed-down cascade for every y - and p_T bin. The Υ production cross section in pPb is scaled with the number of binary collisions from a Glauber calculation.

Cross section for $\Upsilon(1S)$ decays&production in pp collisions at 8 TeV



LHCb data JHEP 2015, 103 (2015)

Fits:

$$\frac{d^2\sigma_{pp}}{dp_{\perp}dy} = \mathcal{N} p_{\perp} \left(\frac{p_0^2}{p_0^2 + p_{\perp}^2} \right)^m \left(1 - \frac{2M_{\perp}}{\sqrt{s}} \cosh y \right)^n$$

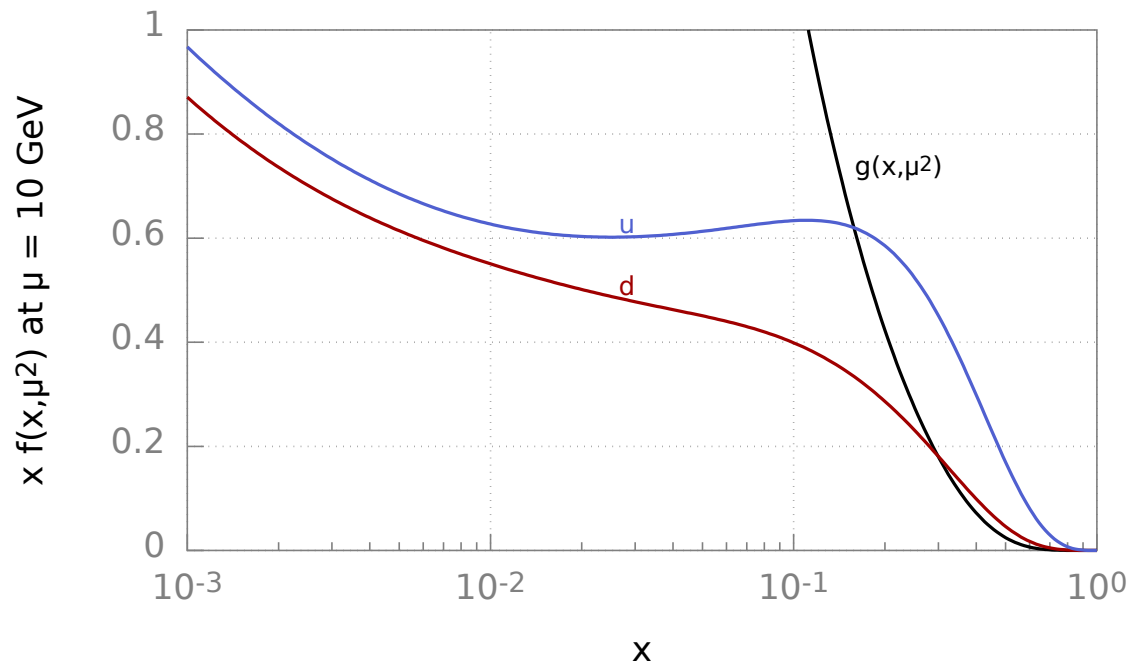
(4 parameters acc. to Arleo et al., JHEP 2013, 155 (2013))

* from inverse feed-down cascade

V.H. Dinh, J. Hoelck and GW,
Phys. Rev. C, in press (2019)

CNM effects: Parton distribution functions (pdfs)

The parton distribution functions (pdfs) define the probability to find a parton i with longitudinal momentum fraction x and factorization scale μ



CT14NLO pdf set for u,d,g

S. Dulat et al., PRD 93, 033006 (2016)

$$x f_g^p(x, \mu^2) \propto x^{-\lambda}$$

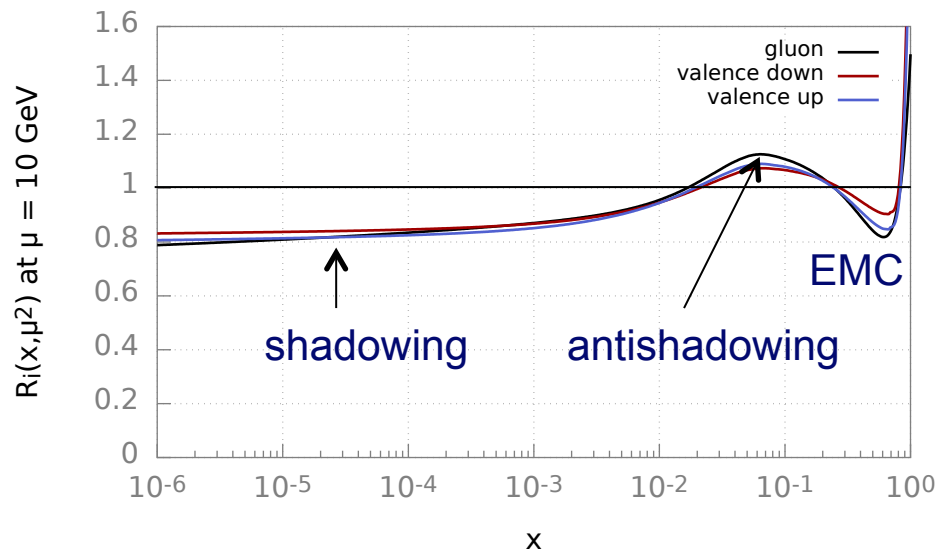
with $\lambda = 0.2 - 0.3$

- Gluon pdfs grow rapidly towards small x
- they are modified by the presence of a nuclear medium

CNM effects: Modified pdfs in the medium - gluon shadowing

Gluonic nuclear modification factors R_g^{Pb} of the gluon pdf in Pb compared to p (main contribution to Υ production arises from gluon fusion)

Nuclear shadowing with EPPS16 pdf set



The bottomonium momentum fraction is given by the kinematics of 2->1 processes

$$x_2(p_{\perp}, y) = \frac{M_{\Upsilon, \perp}}{\sqrt{s_{\text{NN}}}} \exp(-y)$$

$$x_2^{\text{shift}} = x_2(p_{\perp}^{\text{shift}}, y^{\text{shift}})$$

e.g. $x_2 = 2.5 \cdot 10^{-5}$ at $y = 4$, $p_{\text{T}} = 6$ GeV/c

($R_i = 1$ for incoherent superposition of nucleons; x = Bjorken's parton momentum fraction)

CNM effects: Shadowing plus coherent parton energy loss

Including the coherent parton energy loss in the model of Arleo&Peigné, the modification of the Y production cross section from pp to pPb becomes

$$\frac{1}{\langle N_{\text{coll}} \rangle} \frac{d^2\sigma_{\text{pPb}}^{\text{CNM}}}{dp_{\perp} dy} = \int_0^{2\pi} \frac{d\varphi}{2\pi} \int_0^{\varepsilon_{\text{max}}} d\varepsilon P(\varepsilon, E, L_{\text{eff}}) \frac{p_{\parallel}}{p_{\parallel}^{\text{shift}}} \frac{p_{\perp}}{p_{\perp}^{\text{shift}}} R_g^{\text{Pb}}(x_2^{\text{shift}}) \frac{d^2\sigma_{\text{pp}}}{dp_{\perp} dy}(p_{\perp}^{\text{shift}}, y^{\text{shift}})$$

with the shifted quantities

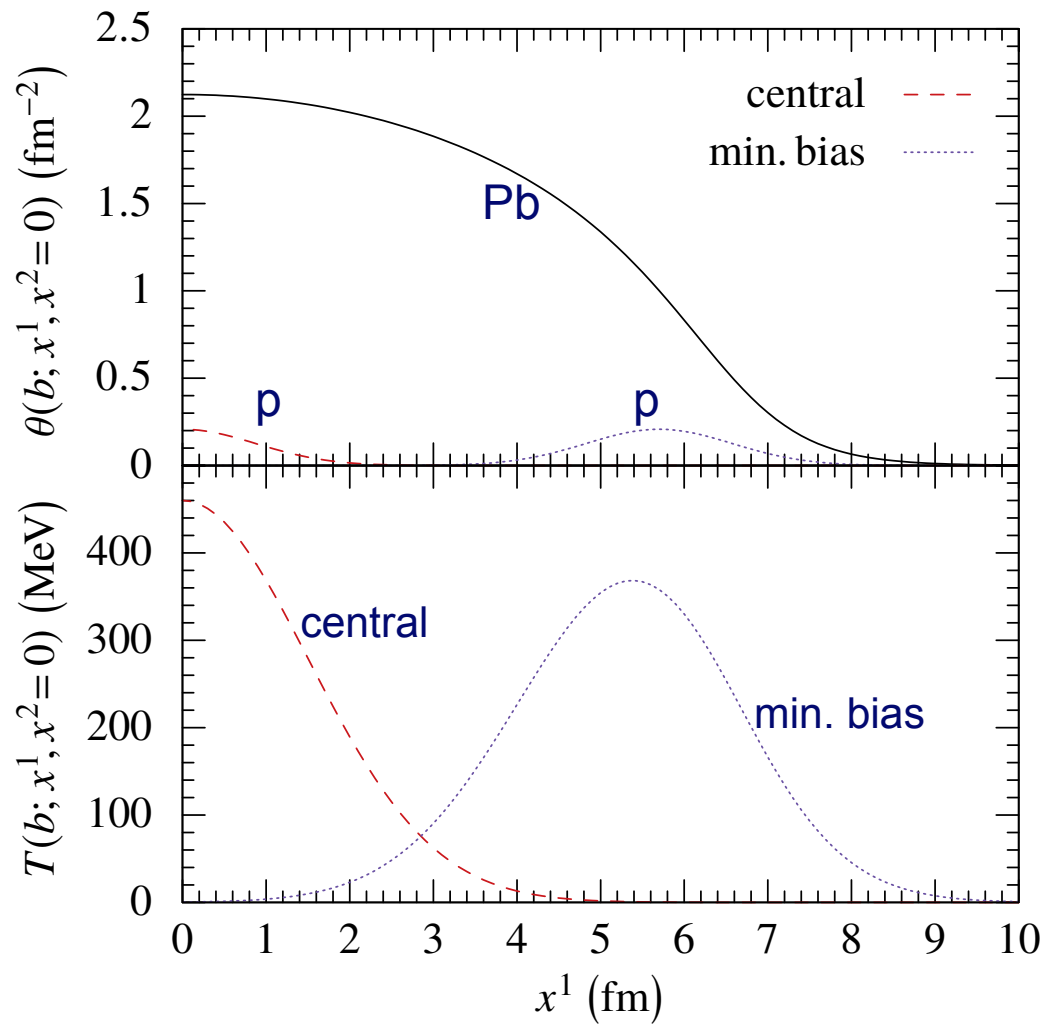
$$y^{\text{shift}} = \text{arcosh} \left[\frac{E(p_{\perp}, y) + \varepsilon}{M_{\perp}(p_{\perp}^{\text{shift}})} \right] - y_{\text{beam}},$$

$$p_{\perp}^{\text{shift}} = \sqrt{p_{\perp}^2 + \Delta p_{\perp}^2 + 2p_{\perp} \Delta p_{\perp} \cos \varphi},$$

$$p_{\parallel}^{\text{shift}} = \sqrt{[E(p_{\perp}, y) + \varepsilon]^2 - M_{\perp}^2(p_{\perp}^{\text{shift}})}.$$

Partons traversing the ('cold') medium loose energy ε via induced gluon radiation
The angle between the Y 's p_{\top} and the transverse momentum kick Δp_{\top} is φ .

QGP effects: Thickness functions and temperature profiles in relativistic pPb collisions



top: thickness functions

$\theta_{\text{Pb}}(x^1, x^2=0)$ for Pb (solid curve),
 $\theta_{\text{p}}(x^1, x^2=0)$ for p

bottom: temperature profiles for
 central (dashed) and minimum-bias
 (dotted) collisions; $T_0 = 460$ MeV

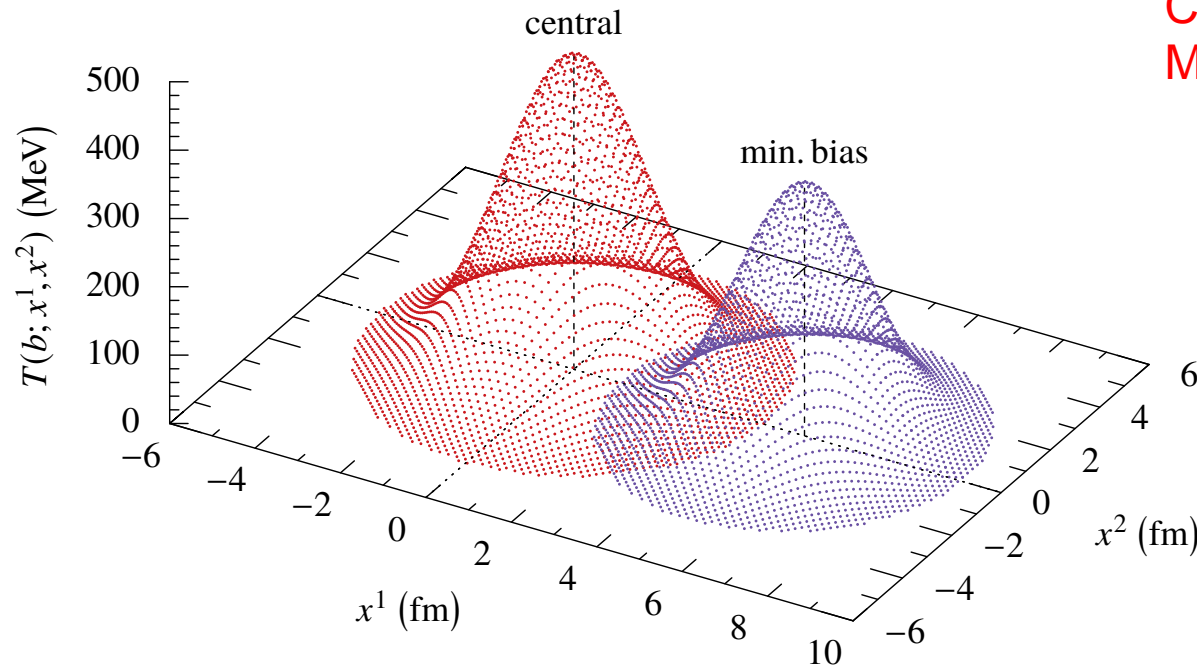
$$T(b; \tau_{\text{init}}, x^1, x^2) = T_0 \sqrt[3]{\frac{\langle n_{\text{coll}} \rangle(b; x^1, x^2)}{\langle n_{\text{coll}} \rangle(0; 0, 0)}}$$

Initial temperature profiles in 8.16 TeV pPb collisions

Transverse plane (x^1, x^2)

Central collisions: $\langle N_{\text{coll}} \rangle \approx 15.6$
 Min. bias: $\langle N_{\text{coll}} \rangle \approx 7$

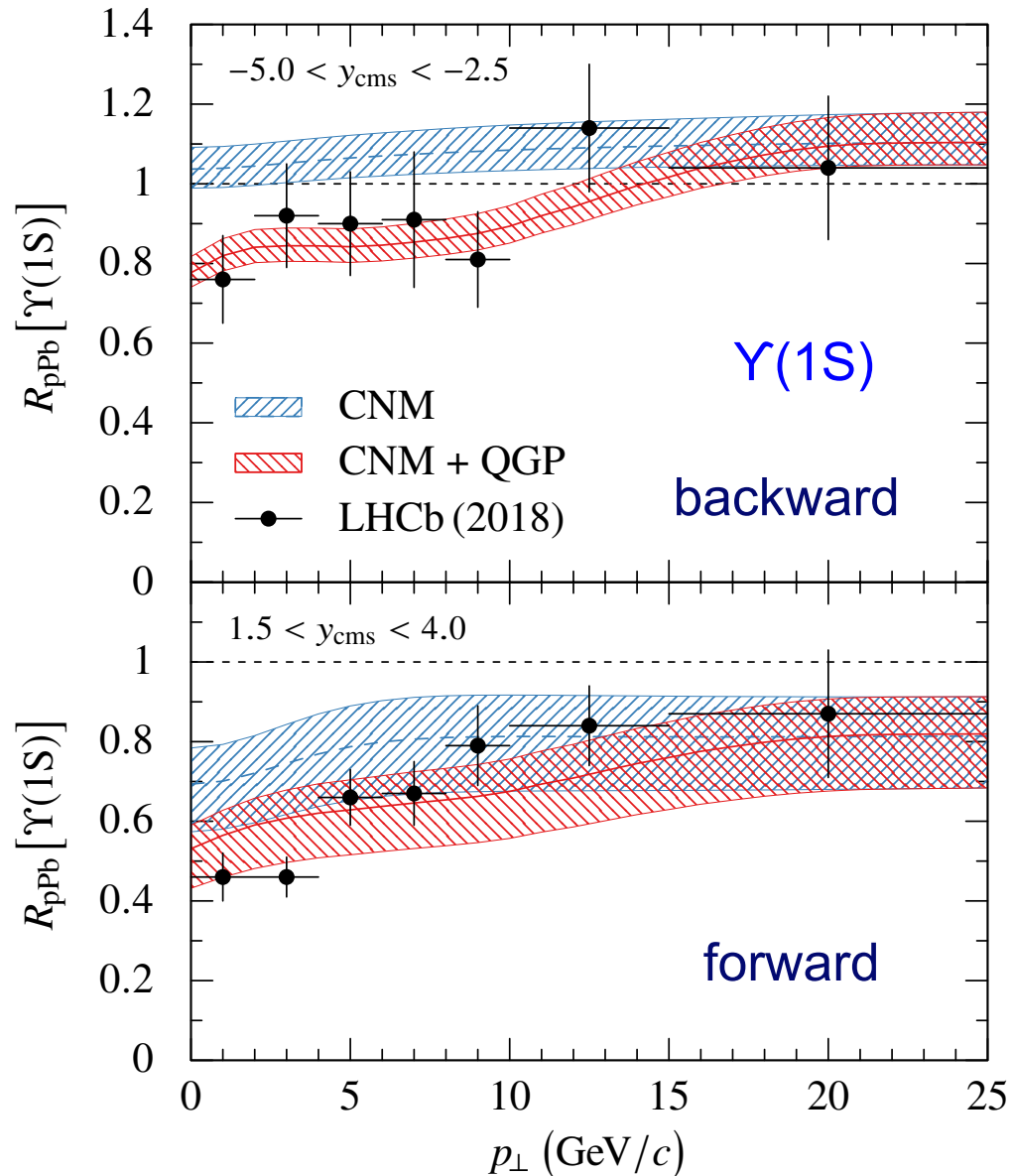
$T_0 = 460 \text{ MeV}$



$$T(b; \tau_{\text{init}}, x^1, x^2) = T_0 \sqrt[3]{\frac{\langle n_{\text{coll}} \rangle(b; x^1, x^2)}{\langle n_{\text{coll}} \rangle(0; 0, 0)}}$$

6. Comparison with LHC data:

Transverse momentum dependence of $\Upsilon(1S)$ yields in pPb at 8.16 TeV vs. LHCb data



Blue: CNM effects only,
backward: antishadowing
forward: shadowing

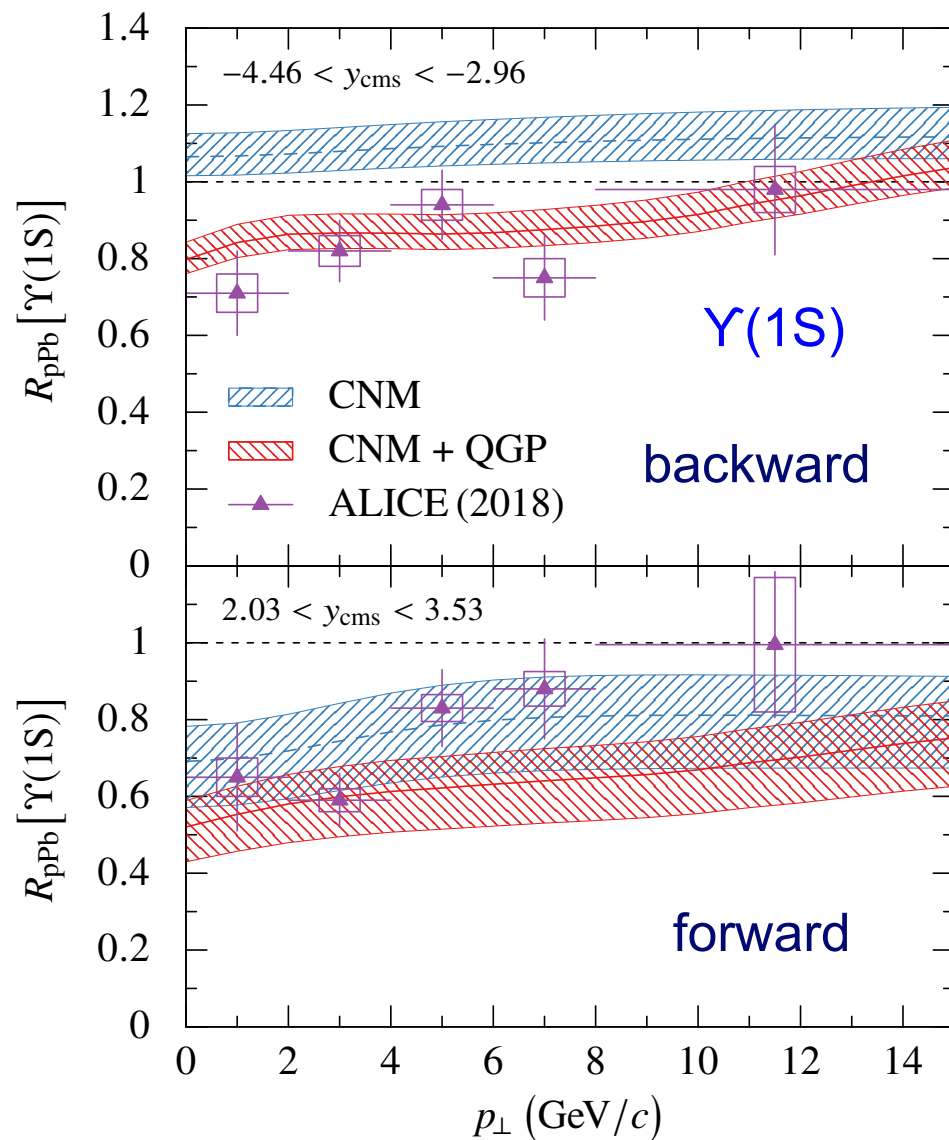
Energy-loss effects pronounced at
 $p_T \leq 8 \text{ GeV}/c$

Red: With hot-medium suppression
($T_0 = 460 \text{ MeV}$; $t_F = 0.4 \text{ fm}/c$)

LHCb data: JHEP 2018, 194 (2018)

V.H. Dinh, J. Hoelck and GW,
Phys. Rev. C, in press (2019)

Transverse momentum dependence of $\Upsilon(1S)$ yields in pPb at 8.16 TeV vs. ALICE data



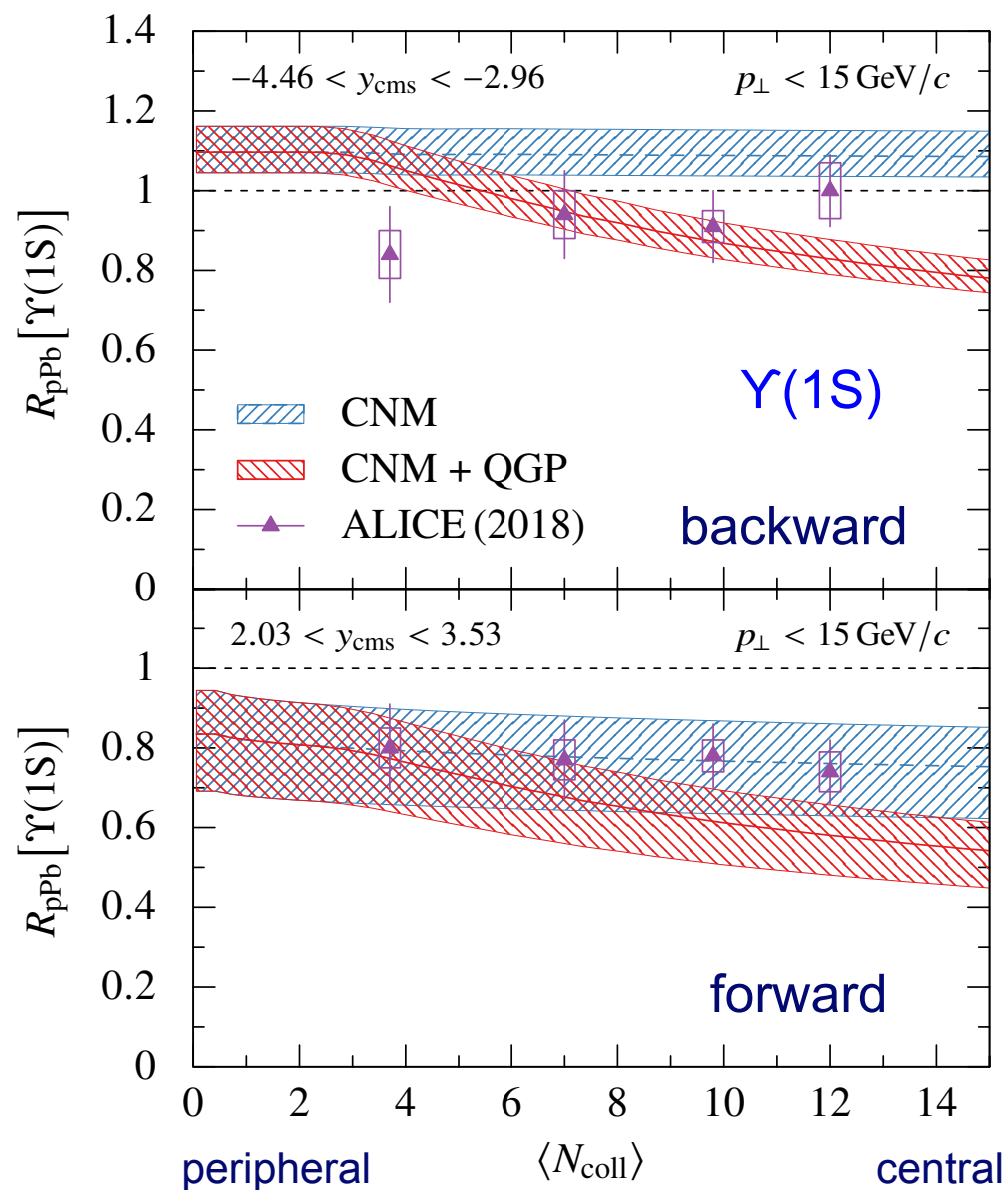
Blue: CNM effects only

Red: With hot-medium suppression

prel. data: ALICE-PUBLIC-2018-008

($T_0 = 460$ MeV; $t_F = 0.4$ fm/c)

Centrality dependence of $\Upsilon(1S)$ yields in pPb at 8.16 TeV vs. ALICE data



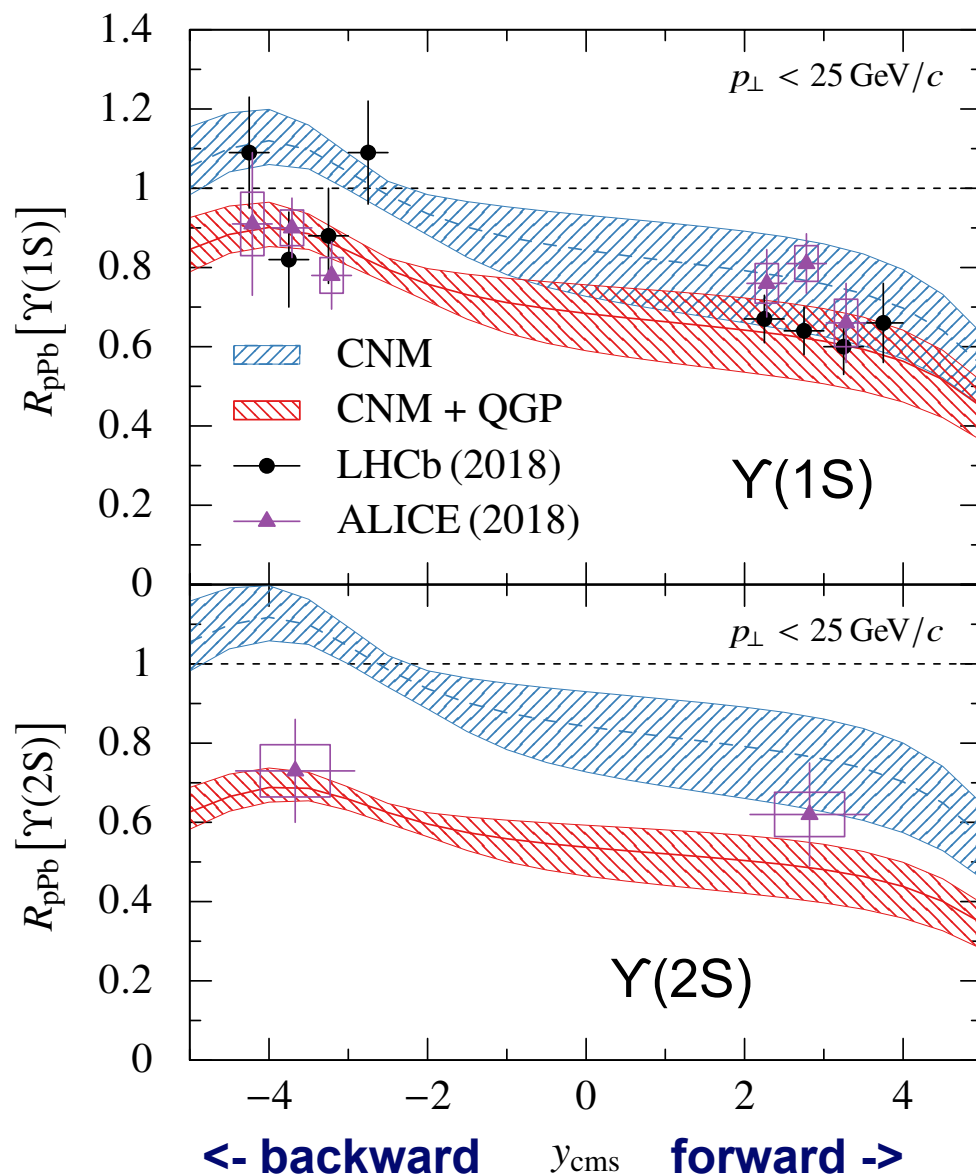
Blue: CNM effects only

Red: With hot-medium suppression

prel. data: ALICE-PUBLIC-2018-008

($T_0 = 460 \text{ MeV}$; $t_F = 0.4 \text{ fm}/c$)

Rapidity dependence of $\Upsilon(1S, 2S)$ yields in pPb at 8.16 TeV vs. LHCb and ALICE data



Blue: CNM effects only

Red: With hot-medium suppression

prel. data: ALICE-PUBLIC-2018-008

data: LHCb: JHEP 2018, 194 (2018)

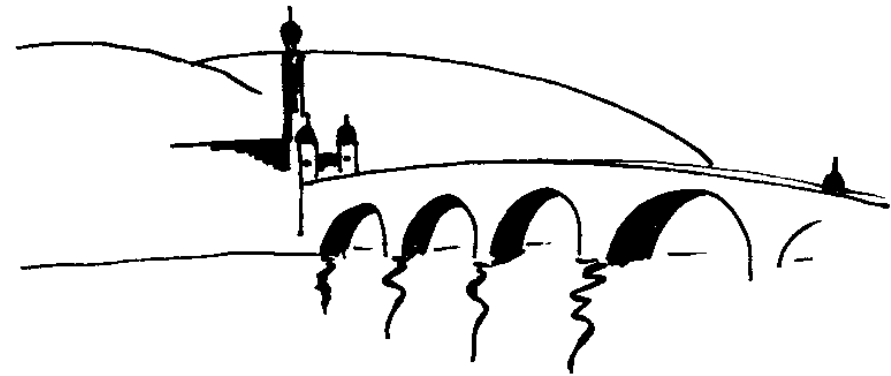
$(T_0 = 460 \text{ MeV}; t_F = 0.4 \text{ fm}/c)$

V.H. Dinh, J. Hoelck and GW,
 Phys. Rev. C, in press (2019);
 arXiv:1903.12594v2

7. Conclusion: Υ in p-Pb @ LHC energies

- The CNM effects shadowing and coherent energy loss are decisive for a proper interpretation of the bottomonia modifications in p-Pb.
- The theoretical model with CNM and **QGP effects** is found to be in agreement with the LHCb and ALICE results for Υ ($1S$) in p_T and rapidity dependence; discrepancies remain for the centrality dependence.
- The hot-medium (QGP) effects play a decisive role in the measured Υ suppression in p-Pb, which cannot be understood with CNM effects alone.
- The initial central temperature of the QGP zone is found to be $T_0 \approx 460$ MeV in 8.16 TeV p-Pb, but depends on the Υ formation time.

Thank you for your
attention !



© H. Schwarz-Köhler

Extra slides: Glauber calculation, number of binary collisions

TABLE II. Results of our Glauber calculation for the expected numbers of binary collisions $\langle N_{\text{coll}} \rangle$ and participants $\langle N_{\text{part}} \rangle$, the differential and integrated inelastic pPb cross sections $d\sigma_{\text{pPb}}^{\text{inel}}/db$ and $\sigma_{\text{pPb}}^{\text{inel}}$, and the corresponding centrality c in pPb collisions at $\sqrt{s_{\text{NN}}} = 8.16$ TeV for different impact parameters b .

b (fm)	$\langle N_{\text{coll}} \rangle$	$\langle N_{\text{part}} \rangle$	$d\sigma_{\text{pPb}}^{\text{inel}}/db$ (fm)	$\sigma_{\text{pPb}}^{\text{inel}}$ (fm ²)	c (%)
0	15.6	16.6	0	0	0
1	15.4	16.4	6.3	3	1.6
2	4.8	15.8	12.6	13	6.0
3	3.7	14.7	18.8	29	13.3
4	2.0	12.9	25.1	52	23.5
5	9.3	10.3	31.4	80	36.6
6	6.0	6.9	37.6	115	52.4
7	2.8	3.6	41.4	155	70.8
8	0.9	1.4	30.6	192	87.7
9	0.2	0.4	11.4	212	96.7
10	0.0	0.1	2.7	218	99.3
11	0.0	0.0	0.5	219	99.9

Bottomonium cross sections in pp and p-Pb

$$\sigma_{pp} = \sum_{ij} \int dx_1 dx_2 f_i^p(x_1, \mu_F^2) f_j^p(x_2, \mu_F^2) \sigma_{ij}(p_1, p_2, \mu_R^2, \mu_F^2),$$

$$\sigma_{pPb} = \sum_{ij} \int dx_1 dx_2 f_i^p(x_1, \mu_F^2) f_j^{Pb}(x_2, \mu_F^2) \sigma_{ij}(p_1, p_2, \mu_R^2, \mu_F^2).$$

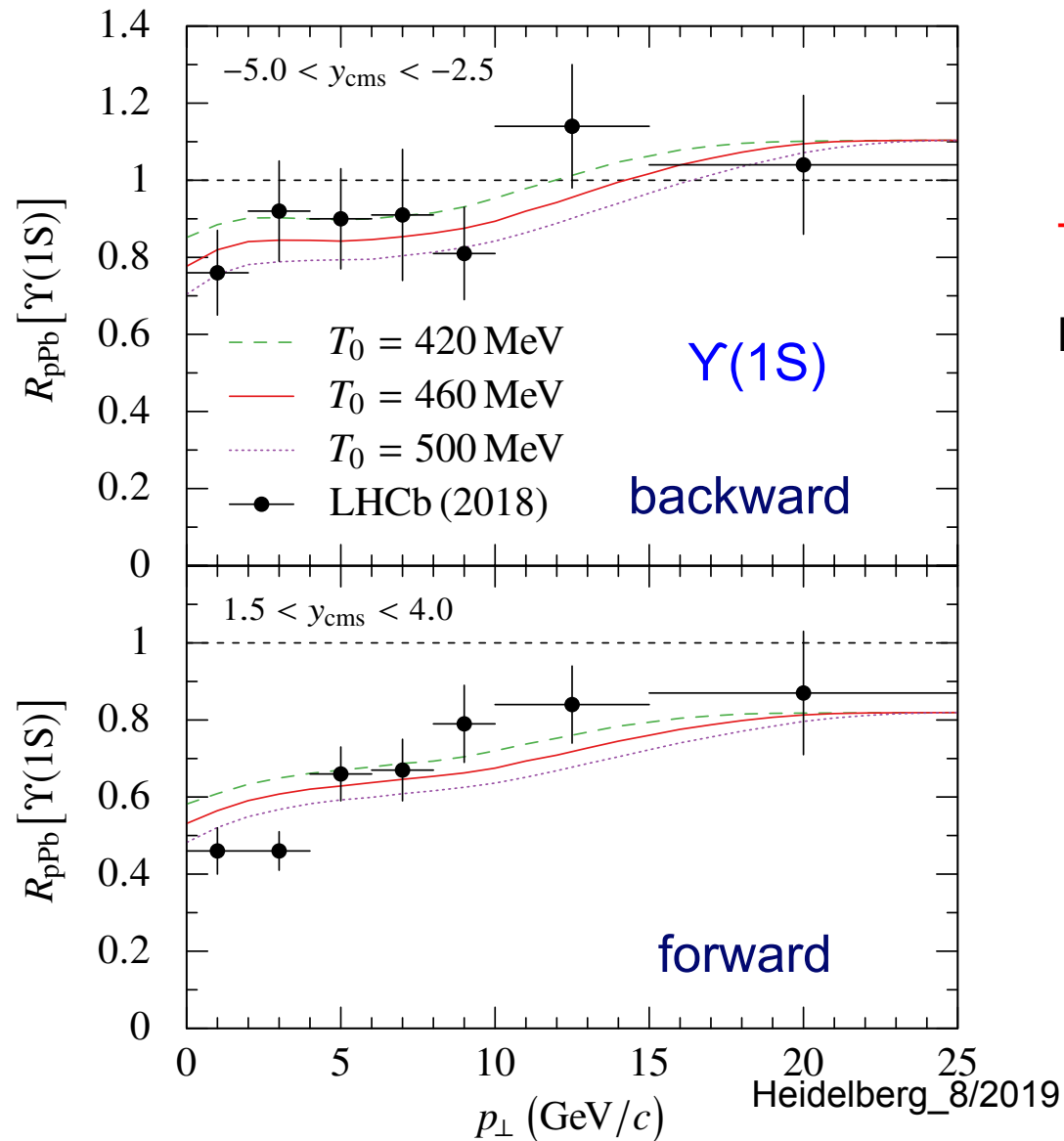
Nuclear modification in Pb parametrized by a shadowing factor

$$R_i^{Pb}(x, \mu_F^2) = \frac{f_i^{Pb}(x, \mu_F^2)}{f_i^p(x, \mu_F^2)} \quad \mu_R \simeq \mu_F \simeq p_\perp$$

For Y production arising from gluon fusion, the diff. cross section in p-Pb becomes

$$\frac{1}{\langle N_{\text{coll}} \rangle} \frac{d\sigma_{pPb}}{dy dp_\perp}(y, p_\perp) = R_g^{Pb}(x_2, \mu_F^2) \frac{d\sigma_{pp}}{dy dp_\perp}(y, p_\perp)$$

Effect of the initial central temperature T_0 :
 Transverse momentum dependence of $\Upsilon(1S)$ yields in pPb at 8.16 TeV



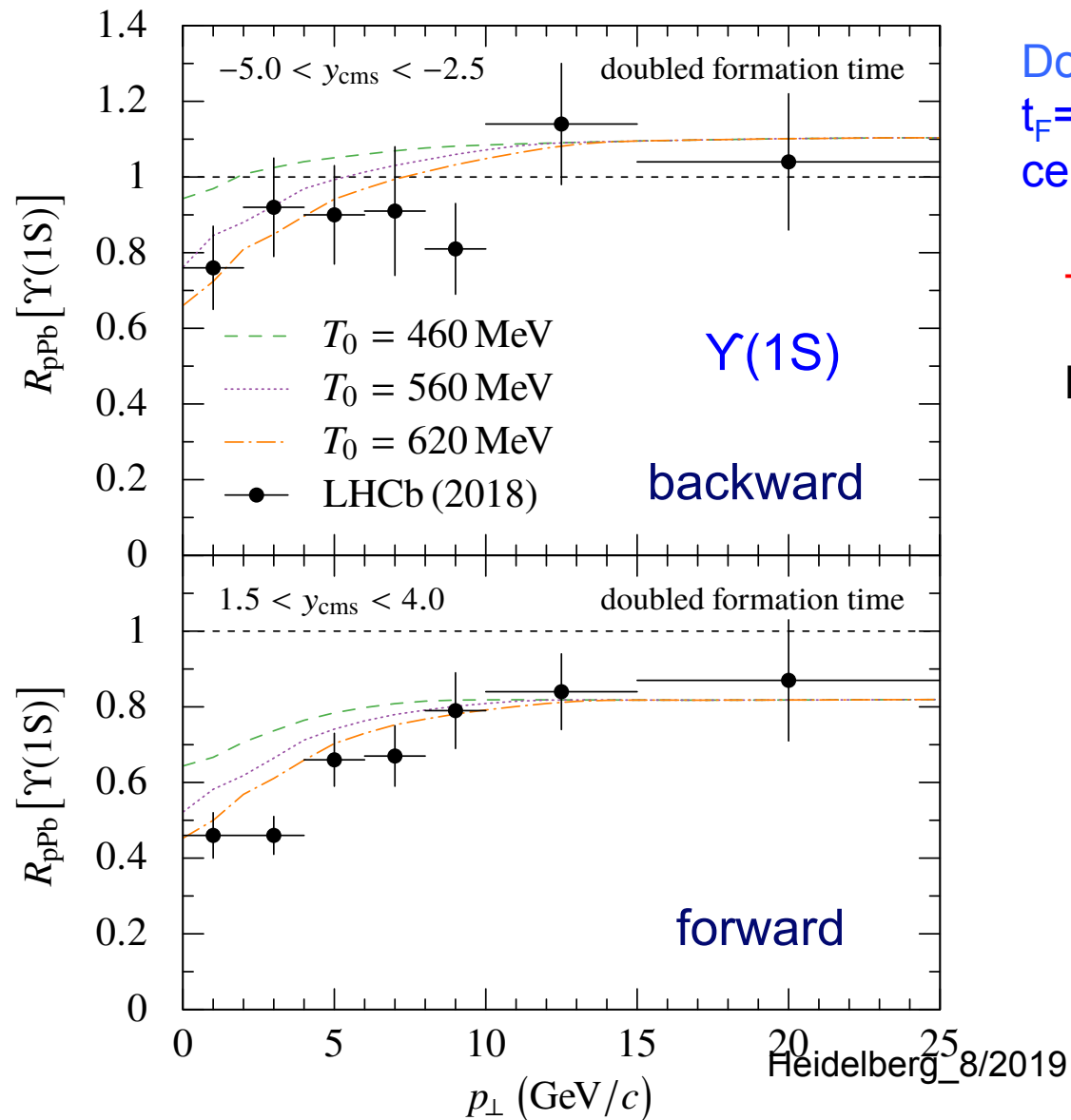
$T_0 = 420, 460, 500$ MeV

LHCb data JHEP 2018, 194 (2018)

($t_F = 0.4$ fm/c)

Effect of the formation time t_F :

Transverse momentum dependence of $\Upsilon(1S)$ yields in pPb at 8.16 TeV



Doubling the formation time to $t_F = 0.8$ fm/c requires larger initial central temperatures:

$$T_0 = 460, 560, 620 \text{ MeV}$$

LHCb data JHEP 2018, 194 (2018)

① , ② Screening and damping in a nonrelativistic potential model

$$V_{nl}(r, T) = -\frac{\sigma}{m_D(T)} e^{-m_D(T)r} - C_F \alpha_{nl}(T) \left(\frac{e^{-m_D(T)r}}{r} + iT\phi(m_D(T)r) \right)$$

$$\phi(x) = \int_0^\infty \frac{dz 2z}{(1+z^2)^2} \left(1 - \frac{\sin xz}{xz} \right), \quad m_D(T) = T \sqrt{4\pi\alpha_s(2\pi T) \frac{2N_c + N_f}{6}}$$

Screened potential: m_D = Debye mass,

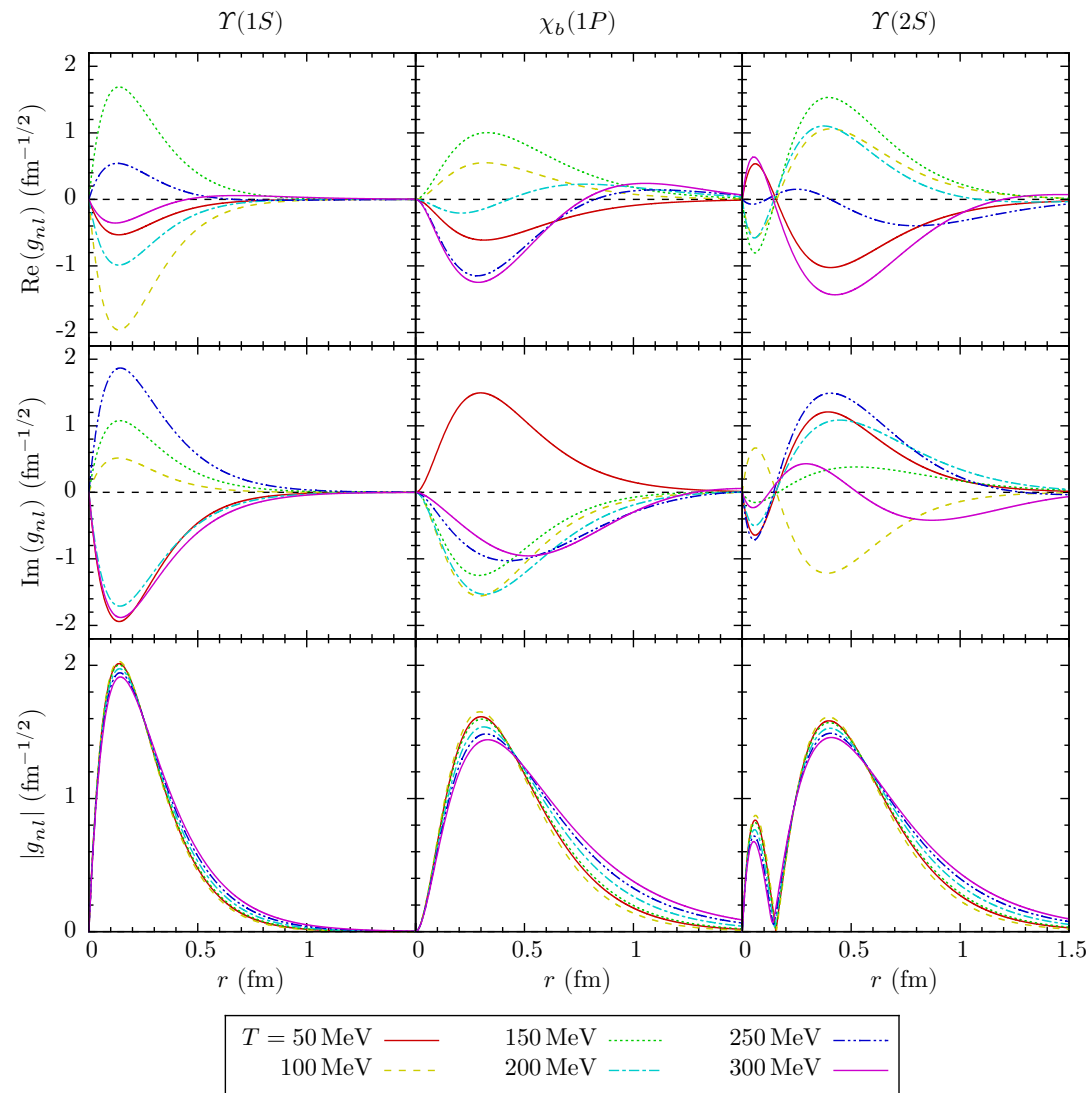
$\alpha_{nl}(T)$ the strong coupling constant;

$$C_F = (N_c^2 - 1) / (2N_c)$$

$\sigma \approx 0.192$ the string tension (Jacobs et al.; Karsch et al.)

Imaginary part: Collisional damping (Laine et al. 2007, Beraudo et al. 2008, Brambilla et al. 2008) for $2\pi T \gg \langle 1/r \rangle$; different form for $2\pi T \ll \langle 1/r \rangle$.

Radial wave functions of $Y(nS)$, $X_b(nP)$ states

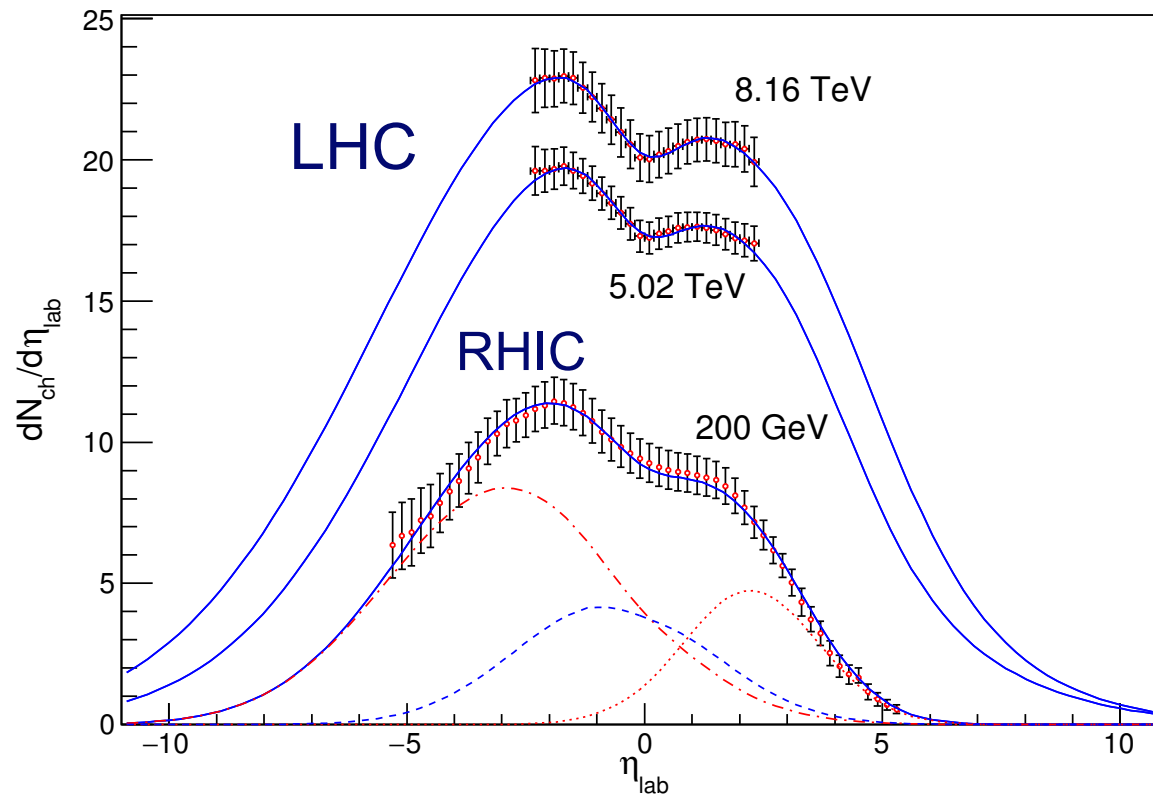


Calculate the damping widths
 $\Gamma_{\text{damp}}(T)$ for all six states

$Y(nS)$, $X_b(nP)$, $n = 1, 2, 3$

Produced charged hadrons in central collisions: 3 sources for particle production

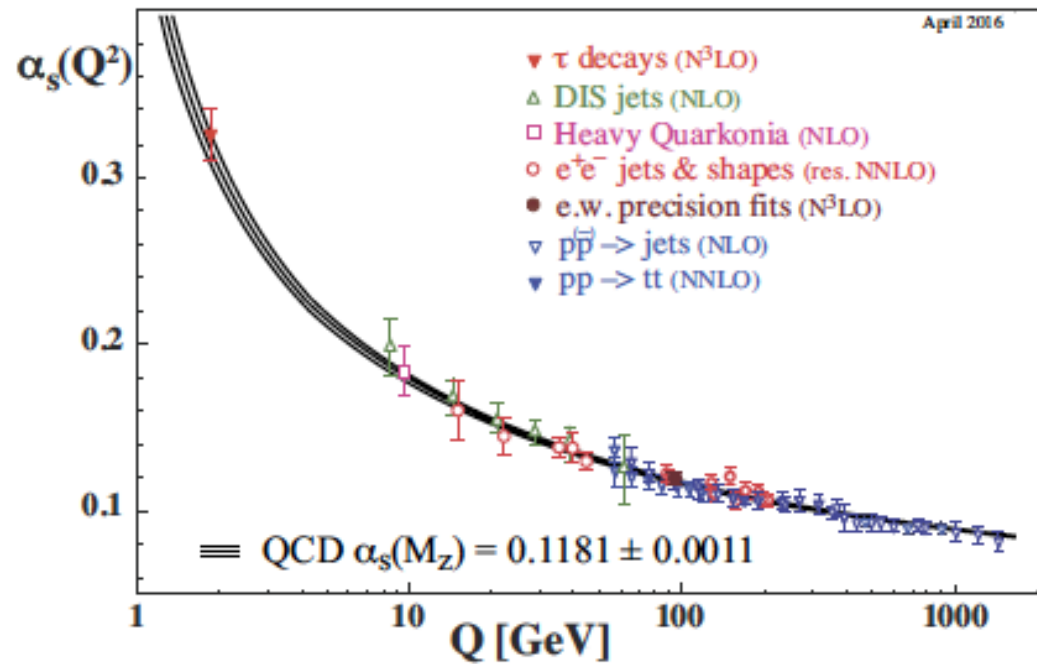
CMS data from min. bias **5.02/ 8.16 TeV p-Pb**,
PHOBOS data from **200 GeV d-Au**



P. Schulz and GW,
MPLA 33, 1850098 (2018);
data from PHOBOS&CMS

$$\eta = -\ln [\tan(\theta/2)]$$

More model ingredients



© K. Bethke 2016

- Consider running of the coupling
- Transverse momentum distribution of the Y included, $\langle p_T \rangle \approx 6 \text{ GeV}/c$
- Relativistic Doppler effect included
- $T_c = 160 \text{ MeV}$

Parameters:

- 1) Y formation time t_F
- 2) initial central temp. T_0

$$\alpha_s(Q) = \frac{\alpha(\mu)}{1 + \alpha(\mu)b_0 \ln \frac{Q}{\mu}}, \quad b_0 = \frac{11N_c - 2N_f}{6\pi}$$

F. Nendzig and GW, J. Phys. G41, 095003 (2014)

$\alpha_{nl}(T) = \alpha_s[\langle 1/r \rangle_{nl}(T)]$ depends on the solution $g_{nl}(r, T)$ of the Schrödinger eq.: Iterative solution

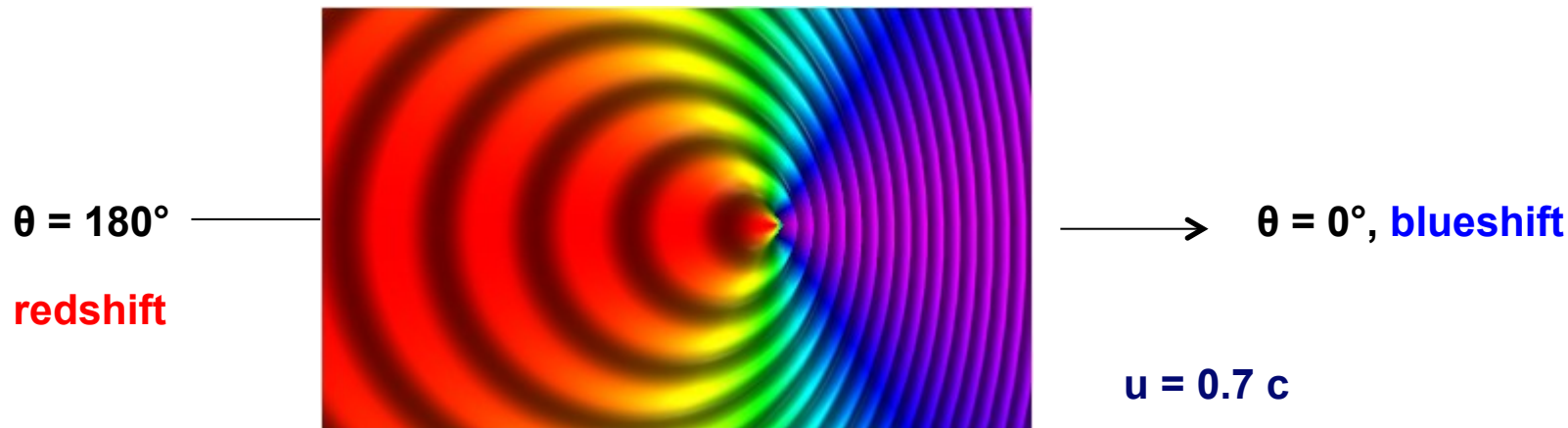
Heidelberg_8/2019

Relativistic Doppler effect

For a finite relative velocity between the expanding QGP and the bottomium states the relativistic Doppler shift results in an angle-dependent effective temperature

$$T_{\text{eff}}(T, \mathbf{u}) = T \frac{\sqrt{1 - |\mathbf{u}|^2}}{1 - |\mathbf{u}| \cos \theta}$$

with the angle θ between the medium velocity \mathbf{u} (in the bottomium restframe) and the direction of the incident light parton. This effective temperature is anisotropic: blue-shifted for $\theta \approx 0^\circ$, red-shifted in the opposite direction.



This has a significant effect on the transverse momentum distributions of the Y's.